Snežana MARINKOVIĆ[1]
Ivan IGNJATOVIĆ[2]
Nikola TOŠIĆ[3]
Jelena DRAGAŠ[4]
Vedran CAREVIĆ[5]

# SUSTAINABLE SOLUTIONS FOR STRUCTURAL CONCRETE – RESEARCH CONDUCTED BY BELGRADE'S CONCRETE STRUCTURES RESEARCH GROUP OVER THE LAST DECADE

**Abstract:** During the last decade, a comprehensive experimental and numerical research on various sustainable concrete options for application in concrete structures was performed at the Faculty of Civil Engineering, University of Belgrade. Several types of green concrete mix designs were investigated: recycled aggregate concrete (RAC), high-volume fly ash concrete (HVFAC), alkali activated fly ash concrete (AAFAC) as well as their combinations. Numerous tests on material physical, mechanical and durability related properties were conducted as well as sustainability assessments of the structural use of such concretes. Structural behavior under short and long-term loading was investigated on full-scale reinforced concrete beams and recommendations for the design of structural members including strength, serviceability and durability were proposed. The work carried out by the group formed a significant part of the basis for RAC provisions in the new Eurocode 2-revision and the fib Model Code 2020.

**Key words:** sustainable structural concrete, properties, structural behavior, design recommendations. Belgrade's Concrete Structures Research Group

# BETON U SVETLU ODRŽIVOG RAZVOJA – ISTRAŽIVANJA BEOGRADSKE GRUPE ZA BETONSKE KONSTRUKCIJE U PROTEKLOJ DECENIJI

**Rezime:** U protekloj deceniji Grupa za istraživanje betonskih konstrukcija na Građevinskom fakultetu Univerziteta u Beogradu je sprovela sveobuhvatna istraživanja različitih vrsta održivih konstrukcijskih betona (betoni na bazi recikliranih agregata – RAC, betoni sa velikom količinom letećeg pepela – HVFAC, alkalno aktivirani betoni – AAFAC, i njihove kombinacije). Istraživanja su sprovedena na nivou svojstava materijala, ponašanja konstrukcijskih elemenata pod krakotrajnim i dugotrajnim opterećenjem i ocene uticaja na životnu sredinu. Na osnovu rezultata eksperimentalnog i numeričkog istraživanja predložene su preporuke za projektovanje, uključujući granična stanja nosivosti, upotrebljivosti i trajnost. Rezultati i preporuke ove Grupe značajno su doprineli formulisanju zahteva za RAC u novoj verziji Evrokoda 2 i u fib Model Code 2020.

**Ključne reči:** održivi konstrukcijski betoni, svojstva, ponašanje konstrukcija, preporuke za projektovanje, Beogradska grupa za istraživanje betonskih konstrukcija

[1] Full professor, Faculty of Civil Engineering, University of Belgrade, Belgrade, Serbia, e-mail: sneska@imk.grf.bg.ac.rs
[2] Associate professor, Faculty of Civil Engineering, University of Belgrade, Belgrade, Serbia, e-mail: ivani@imk.grf.bg.ac.rs
[3] Dr, Civil and Environmental Engineering Department, Universitat Politècnica de Catalunya, Barcelona, Spain, nikola.tosic@upc.edu
[4] Assistant professor, Faculty of Civil Engineering, University of Belgrade, Belgrade, Serbia, e-mail: jelenad@imk.grf.bg.ac.rs
[5] Assistant professor, Faculty of Civil Engineering, University of Belgrade, Belgrade, Serbia, e-mail: vedran@imk.grf.bg.ac.rs

## 1. INTRODUCTION

A key challenge of this century is the need to mitigate and adapt to climate change, and avoid negative impacts on social well-being, the economy and the environment. Across the globe, climate change has already altered hydrological and natural systems, generated net negative effects on crop yields, and increased the frequency of climate-related extremes [1]. Such negative impacts are set to continue: e.g. higher risks from natural hazards, global sea rise, significant species loss, ocean acidification, etc [2]. To avoid the worst, it is imperative to "hold the increase in the global average temperature to well below 2°C above pre-industrial levels and to pursue efforts to limit the temperature increase to 1.5°C above pre-industrial levels" [3] – the main objectives of the flagship Paris Climate Agreement (COP 21).

Achieving results with the urgency needed to meet COP 21 commitments requires targeting high-emitting industries and activities. The construction industry – including a range of activities from the extraction of raw materials; manufacturing/distribution of construction products; construction, management, control of construction works; maintenance, renovation and demolition of buildings; and recycling construction and demolition waste [4] – is alone responsible for a large portion of Europe's environmental footprint: 50% of natural raw materials use, 40% of total energy consumption [5] (as the single largest consumer), 46% of total waste generated (construction and demolition waste – CDW) [6], and 36% of all greenhouse gas (GHG) emissions [7].

Within the construction industry, concrete and other cement-based materials are ubiquitous, and are responsible for a large share of the industry's environmental impacts. Concrete is the second most-used material in the world, after water, with 25 billion tones are produced annually [8]; it is mainly composed of cement, water and aggregates (Figure 1). Due to cement's production process and the chemical reactions involved, it is responsible for 7–10% of annual anthropogenic $CO_2$ emissions [9].

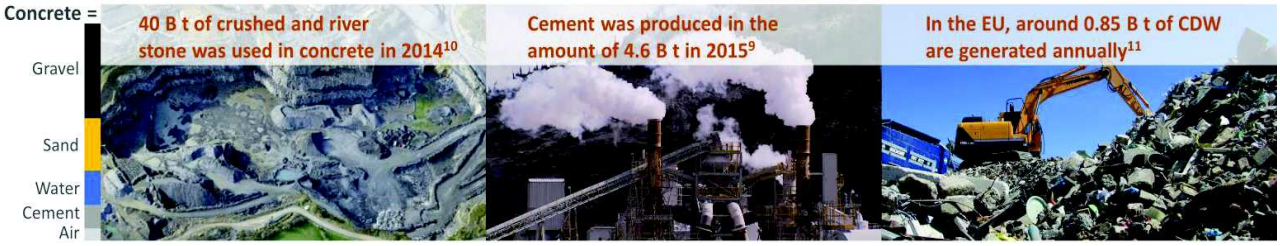


*Figure 1 – Environmental impacts of concrete production and construction*

For these reasons it is of crucial importance to find way(s) of greening the concrete industry, i.e. to decrease its impact on the environment. These efforts can be divided into three major groups: (1) recycling of construction and demolition waste as a way to reduce the amount of waste and consumption of natural resources, (2) on the material level by introducing green concretes, and (3) on the structural level, by design for longer service life and reuse. Green concretes are developed mainly by replacing natural with recycled aggregates and cement with supplementary cementitious materials (SCM) with low embodied $CO_2$. The most common SCMs are reactive wastes from other industries; for instance, fly ash, the by-product of the electricity production in coal-burning power plants, and granulated blast furnace slag, the by-product of pig-iron production in blast furnaces. Fillers, inert or weakly reactive fine particulate materials, can partially replace cement or other reactive SCMs; the most commonly used is limestone filler. At the end of this 'cement replacement' line stands alkali activated concrete in which the cement binder is completely replaced by alkali activated materials rich in silicon and aluminium. Different natural and waste materials are activated with alkaline solutions, usually with a combination of sodium hydroxide and sodium silicate solutions. If low calcium FA is used, such concrete is named alkali activated fly ash concrete, which uses caustic sodium hydroxide and usually needs curing at elevated temperatures.

During the last decade, a comprehensive experimental and numerical research on various sustainable structural concrete solutions was performed by Concrete Structures Research Group at the Faculty of Civil Engineering, University of Belgrade. Several types of green concrete mix designs were investigated: recycled aggregate concrete (RAC), high-volume fly ash concrete (HVFAC), alkali activated fly ash concrete (AAFAC) as well as their combinations. Numerous tests on material physical, mechanical and durability related properties were conducted as well as sustainability assessments of the structural use of such concretes. Structural behaviour under short and long-term loading was investigated on full-scale reinforced concrete beams and recommendations for the design of structural members including strength, serviceability and durability were proposed. The work carried out by the group formed a significant part of the basis for RAC provisions in the new Eurocode 2-revision and the fib Model Code 2020. Herein, the most important research results are presented.

## 2. RECYCLED AGGREGATE CONCRETE – PROPERTIES AND STRUCTURAL BEHAVIOUR OF BEAMS UNDER SHORT-TERM LOADING

### 2.1. Recycled aggregate concrete

One of the solutions to the problems related to disposal of construction and demolition waste and depletion of natural resources of aggregates is recycling of deposited building materials, primarily concrete. It can be processed so to obtain the recycled concrete aggregate (RCA) for various applications. Although primarily focusing on structural elements made of recycled aggregate concrete [10], starting points for investigation were characterization of RCA [11] and investigation on physical and mechanical properties of RAC [12]. Of course, critical analysis of data from the literature, collected and organized in the form of operational database had been done even before. The relationship between certain properties of RAC (compressive strength, tensile strength, modulus of elasticity [13], creep [14], shrinkage [15]) and RCA amount, the influence of different parameters (water to cement ratio, quality of parent concrete, supplementary cementitious materials) to the properties of RAC and the state-of-the-art of technical legislative regarding the use of RCA and RAC, were the main outcomes from that analysis [11]. Literature review also included aspects of sustainability [16-18], recycling technology [19], microstructure and durability [20]. Numerous of testing at material level and improving the procedure of RAC design for the target compressive strength [21] have been performed prior to full scale RAC beams testing.

Experimental evidence on the RAC structural behavior is very important because it is difficult to predict the impact of RAC properties on the overall reinforced concrete elements behavior based only on those test results obtained from material properties. The aim of the research was to widen the existing experimental database on the flexural and shear behaviour of reinforced RAC beams [22,23] in favor of the idea of using recycled aggregate concrete in structural concrete elements (beams). The objective was also to determine whether code equations for NAC are applicable for the prediction of ultimate strength of RAC beams and parameters of serviceability limit state [24], based on the comparison with different codes and including test data available in literature.

### 2.2. Experimental research

The methodology of experimental research is based on the comparison of the flexural and shear performance of reinforced concrete beams made of natural aggregate concrete (NAC) and recycled aggregate concrete [25,26]. Three different replacement ratios of coarse NA with coarse RCA (0%, 50%, and 100 %), three different tensile reinforcement ratios (0.28%, 1.46% and 2.54%) and three different shear reinforcement ratios (0%, 0.14%, and 0.19 %) were the main parameters in this two-phase study. First, full-scale tests up to failure load on 9 simply supported beams were conducted in order to investigate the flexural behavior of RAC beams, where all NAC and RAC concrete mixtures were designed to have the same cube compressive strength of 42 MPa and the same workability defined by slump of 8±2 cm after 30 minutes. The second phase was comparison of

structural responses of NAC and RAC beams prior to shear failure, where the target compressive strength was 40 MPa and the same workability like in case of flexural testing. All the beams were simply supported with a span of 3.0 m and subjected to four-point load system. A shear span-to-depth ratio of 4.0 was kept constant for beam specimens in the first phase (flexure) and 4.2 in the second phase (shear). Recycled concrete aggregate for RAC mixture design and preparation was obtained from mixed concrete rubble, with water absorption between 3.7% and 4.6% for different grain size categories and that was the only RCA property that is significantly different from natural aggregate.

### *2.2.1. Flexural behaviour*

The test set-up and measuring equipment is presented in Fig. 2. Strains in tensile reinforcement were measured by means of electronic resistance strain gauges (SSG), while vibrating wire strain gauges (VWSG) were used to measure concrete's strains. Beam deflections were measured by linear potentiometers (LP) placed at the supports and at each 50 cm along the beam, Fig. 2.

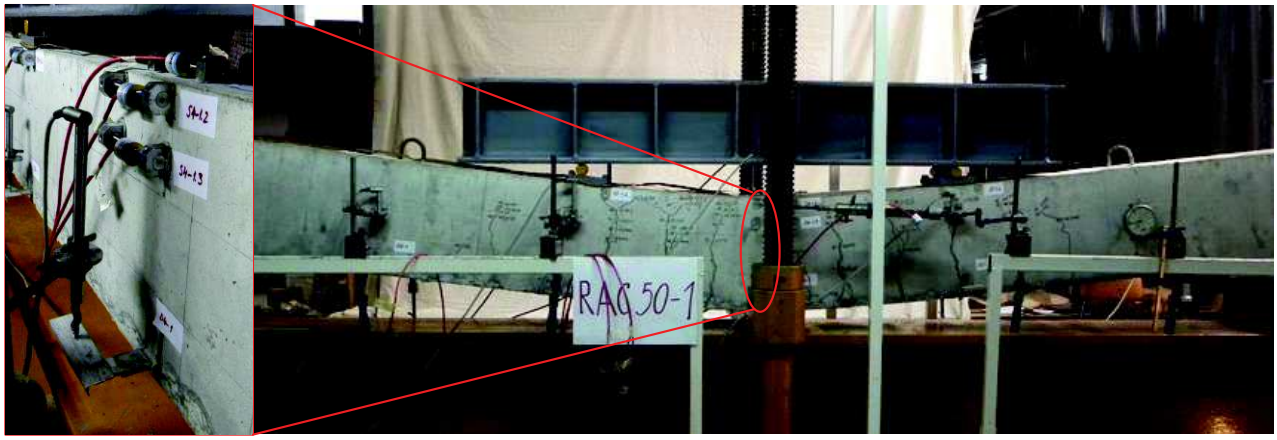


*Figure 2 – Experimental set-up for beam testing in flexure*

The load (2P) - deflection (δ) curves of the beams with different reinforcement ratios and concrete types are shown in Fig. 3. Three types of failure can be seen, from ductile to brittle, dominantly defined by the amount of reinforcement and independently of the concrete type. There are only slight differences in failure load ($\Delta 2P_u$) as well as in ductility within the groups of beams with the same reinforcement ratio, regardless of the concrete type.

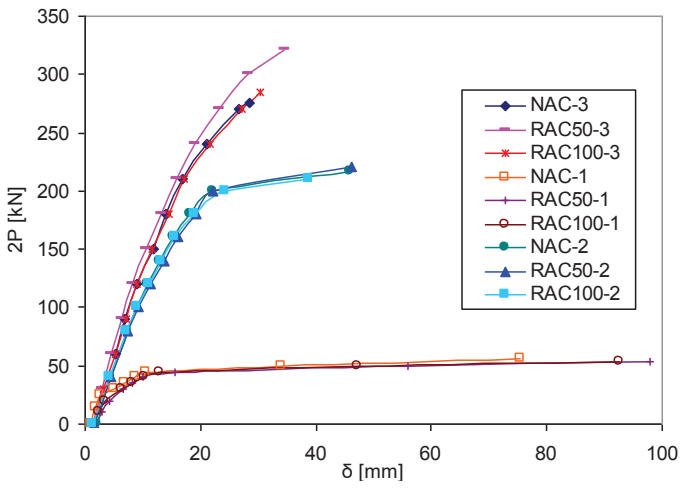


*Figure 3 – Load–deflection curves*

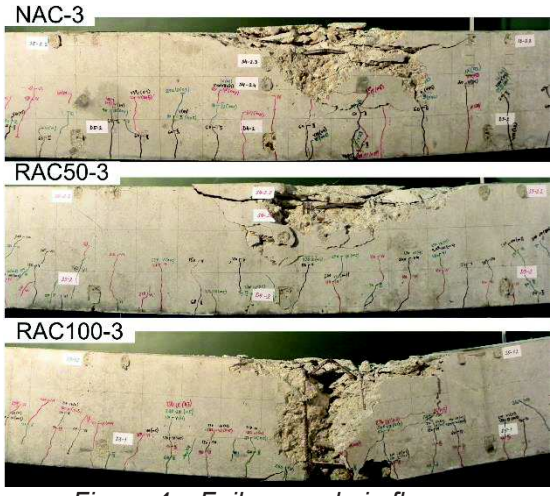


*Figure 4 – Failure mode in flexure*

The most important difference in the failure mode of the beams with different types of concrete was in the scale of concrete damage at failure. With the increase in recycled aggregate content, the size of failure surface and the level of the concrete destruction increased. Unlike the beam NAC-3,

concrete in RAC100-3 beam was broken into small particles at failure, being reduced almost to the size of aggregate, Fig. 4. While the cracks in NAC-3 beam formed a well-known cone, beam RAC100-3 exhibited the most destructive failure, with excessive rotation and large deterioration of the mid-span section – the loss of the whole section was observed, Fig. 4. The explanation lays in the new interfacial transition zone between RCA and the new cement paste which is usually porous and loose, and forms a weak link in RAC. However, similar behaviour at failure between NAC-3 and RAC50-3 proved that substitution of 50% of natural coarse aggregate with recycled one is feasible even at macro level and without negative consequences on the structural behaviour up to the failure.

Structural behaviour at the service load was quite similar for the group of beams reinforced with the average and maximum reinforced ratios (deflection, crack spacing and crack width), while the late formation of the first crack in NAC beam with minimum amount of steel resulted in smaller deflection compared to the other under-reinforced beams (RAC50-1 and RAC100-1), Fig. 5.

In order to extend the conclusion of the own experimental investigation, analysis of other results from the literature was conducted. Summarized conclusion is that compared to control NAC beams, RAC beams made of concrete with the same water-to-cement ratio and replacement ratio of natural with recycled coarse aggregate up to 100%, have: 10% lower cracking load, 13% higher service deflection and practically the same flexural capacity on average as corresponding NAC beams, Fig. 6.

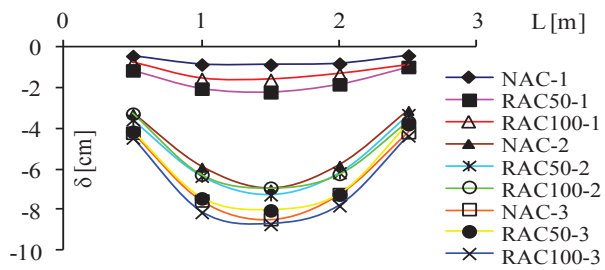


*Figure 5 – Load–deflection curves*

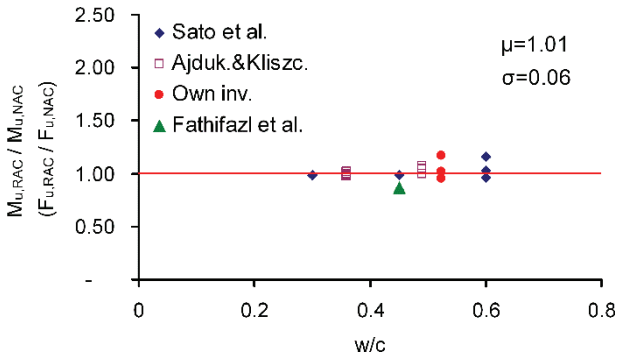


*Figure 6 – Ultimate moment of NAC and RAC beams*

### *2.2.2. Shear behaviour*

The test set-up and measuring equipment is presented in Fig. 7. There were a couple of SSGs on each of the four stirrups in the left shear span of beams with minimum shear reinforcement and on each of the six stirrups in beams with a higher percentage of shear reinforcement. Pairs of VWSGs with a 100 mm base were mounted at the upper surface of each beam. Beside this, the strain rosettes were placed in the middle of the shear span where the passing of the critical inclined crack was expected, Fig. 7. They were formed from three LPs with an angle of 60º between each and with a base of 150 mm.

Shear failure modes of RAC beams without shear reinforcement did not differ from the failure mode of NAC beam, but slightly different angle and shape of the shear crack was observed, Fig. 8. Instead of a pure diagonal crack as in beam NAC-1, the 'S' crack appeared in RAC beams where the crack angle in the middle third was about 45° but only about 15° in other parts connecting the load and support zone, Fig. 8.

The difference in the shape of the cracks in RAC and NAC beams was dominantly caused by the different angle of the mid part of the crack (in the middle third of the beams height) while the other two thirds were formed in an expected manner. The angle of the first crack was determined by the direction of the principle tensile stress calculated from the measured strains in the rosette (Fig. 7). It turned out that the angle of principle tensile stress in beam NAC-1 was 35° while in RAC50 and

RAC100 beams it was 44° and 43°, respectively, and they correlated with the crack angles noticed during the experiment. In general, beams with shear reinforcement showed similar behaviour under loading, proved by the similar data regarding the deflections, concrete and reinforcement strains, Fig. 9. Almost all stirrups in all tested beams reached at least yielding strain at the failure load. This point to a similar contribution of the shear reinforcement and a similar contribution of the aggregate interlock in the shear transfer mechanism of NAC and RAC beams with shear reinforcement. The failure mode in all six beams with stirrups, irrespective of concrete type, was a brittle one in the direction of the main diagonal crack and marked with crushing of concrete in the vicinity of the load. Differences in normalized shear strengths of beams with 0%, 50% and 100% of RCA and the same amount of shear reinforcement were limited to 5%.

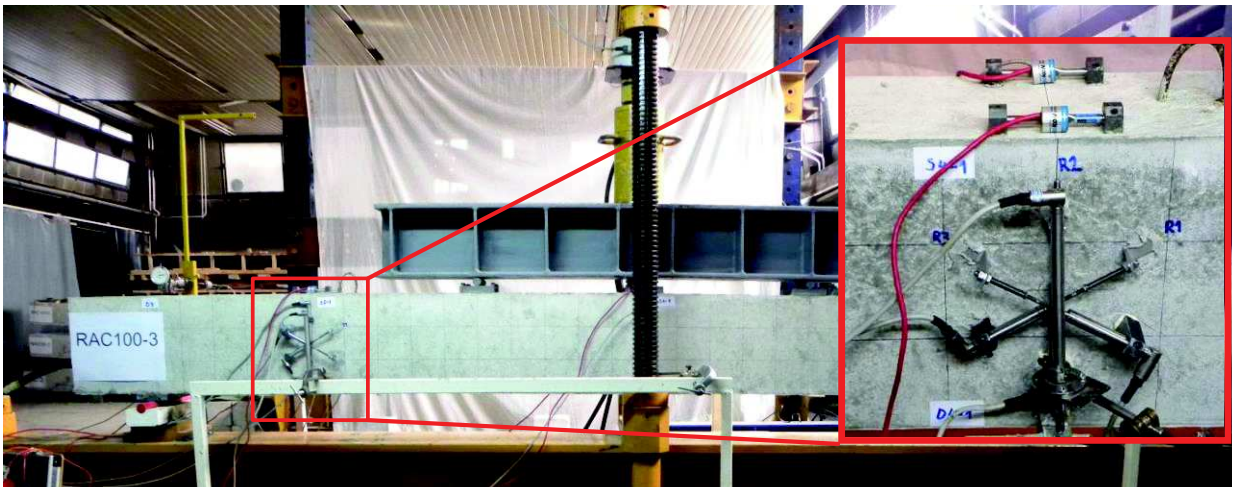


*Figure 7 – Experimental set-up for beam testing in shear*

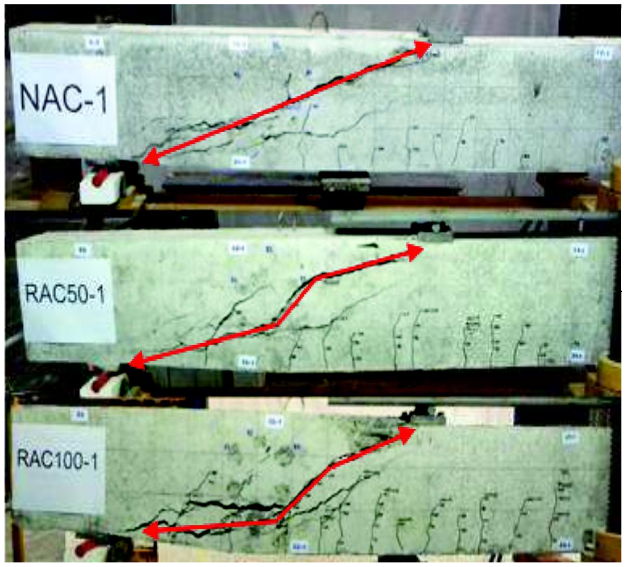


*Figure 8 – Distribution of cracks prior to shear failure*

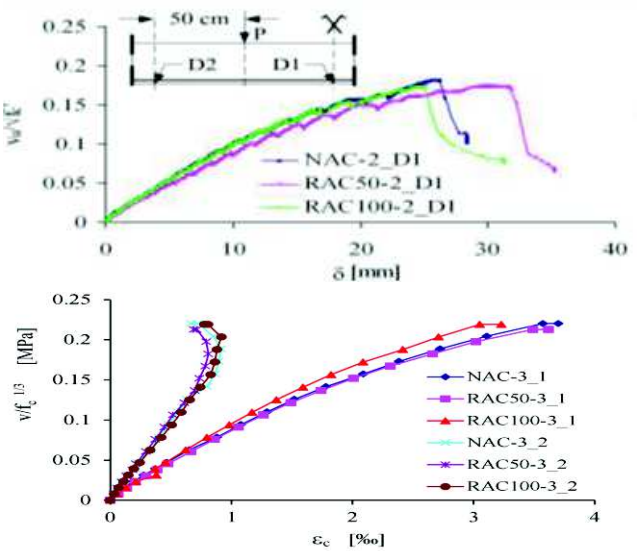


*Figure 9 – Deflection and concrete strains*

At the load step when the first shear crack was noticed by naked eye, principal tensile stress between 15 MPa and 20 MPa was calculated for all beams (Fig. 10) and that is, of course, impossible having in mind the concrete tensile strength. Thus, the difference between what we can see during the experiment (‘first’ shear crack formation) and what we cannot see (internal structural damage) but can be measured, must be emphasized and this is an example. The internal structural damage, i.e. formation of internal micro cracks, obviously occurred in all three beams several load steps prior to ‘first’ shear crack formation and can be caught as the rapid increase of principle strains which occurred three load steps before the crack was noticed at the surface of the beam, Fig. 10.

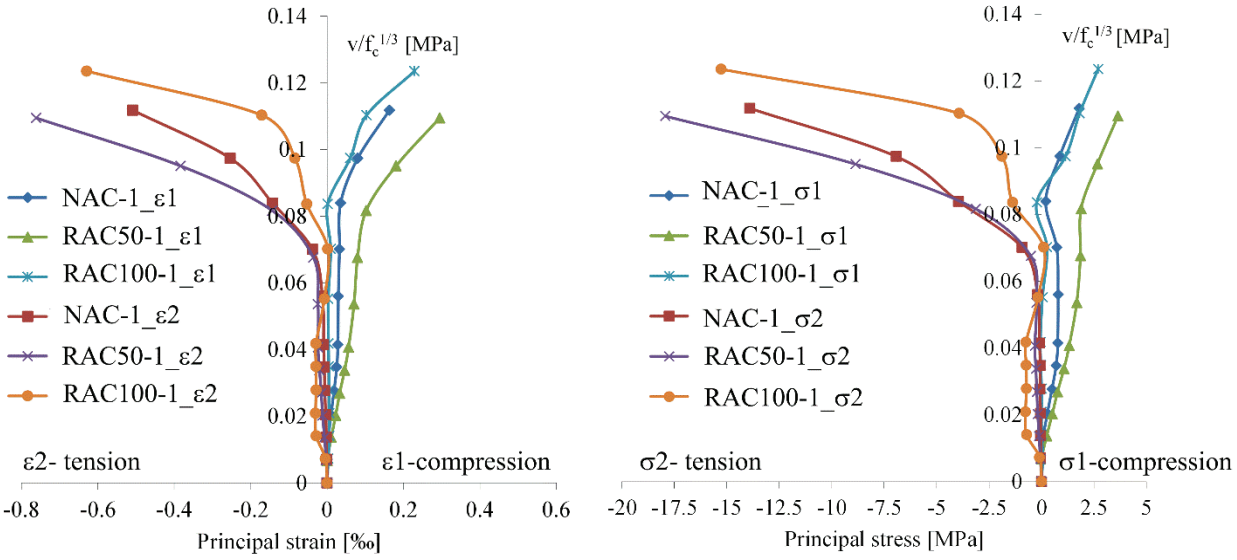


*Figure 10 – Principal strain and stress for NAC and RAC beams*

The applicability of different code provisions for the shear strength predictions of RAC beams with and without shear reinforcement was tested based on own and other test results. The average value of the $V_{u,test}/V_{u,code}$ ratio is similar for RAC100 and RAC50 beams without shear reinforcement, and 5% to 6% lower than for NAC beams, regardless of the analyzed code. In case of beams with stirrups, the predictions are very conservative with relatively high coefficients of variation for all types of concrete, especially according to EN 1992-1-1 [27]. The best prediction of the ultimate shear load was obtained by ACI 318M-14 specifications [28].

## 3. TIME-DEPENDENT BEHAVIOUR OF RECYCLED AGGREGATE CONCRETE

Beside short-term material and structural behaviour of RAC, an important topic that was investigated was the time-dependent behaviour of RAC, i.e. its long-term deformation. In this regard, research focused on experimental and analytical investigation into the shrinkage and creep of RAC as well as the deflection behaviour of reinforced RAC members.

### 3.1. Experimental research

From 2015 to 2017, an experimental programme was carried out at the University of Belgrade's Faculty of Civil Engineering into the time-dependent behaviour of RAC and reinforced RAC beams [29,30]. For the purpose of this campaign, NAC and RAC with 100% of coarse RCA (with a water absorption of 3.3%) were prepared with similar compressive strengths (40.7 and 37.4 MPa, respectively) and shrinkage, creep and deflections were tested during 450 days. In terms of material properties, approximately 20% higher shrinkage was observed for RAC than for NAC, in line with previous literature reviews [31,32].

Creep was tested only on RAC by applying load on concrete prisms through a lever mechanism (Figure 11a) at 7 and 28 days. The load was applied so that the achieved stress-to-strength at loading ratio $\sigma_c(t_0)/f_{cm}(t_0)$ was 0.60 and 0.45 for loading at 7 and 28 days, respectively. Higher values of creep strains were observed for specimens loaded at 7 days, but the time evolution of creep did not indicate any effect of loading age, i.e. no nonlinear or tertiary creep was observed (Figure 11b).

In terms of structural behaviour, two NAC and two RAC beams were tested. The tested beams had a 160/200 mm cross-section and a 3200 mm span and were tested in four-point bending during 450 days. The beams had a reinforcement ratio of 0.58% with 2Ø10 mm bars in tensions and 2Ø6 mm bars in compression with Ø6 mm stirrups, Figure 12. One pair of NAC and RAC beams was loaded

at 7 days and the other pair at 28 days so that for the beams loaded at 7 days, the $\sigma_c(t_0)/f_{cm}(t_0)$ ratio was 0.60 and for the beams loaded at 28 days 0.45.

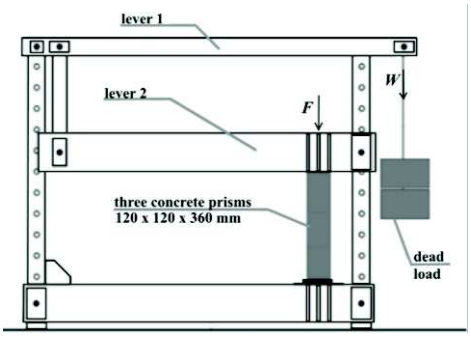


*Figure 11a – Steel frames for measuring creep [30]*

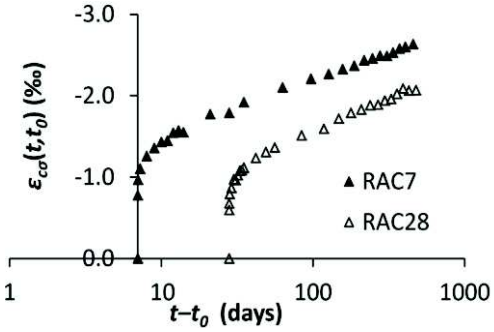


*Figure 11b – Stress-dependent RAC strains [30]*

The concretes had similar mechanical properties: compressive strengths of 40.7 and 37.4 MPa for NAC and RAC, respectively, with moduli of elasticity of 32.2 and 30.8 GPa, respectively and tensile strengths of 2.4 and 2.5 MPa, respectively. In terms of result, the normalized deflections, i.e. the $a_t/a_0$ ratio showed no differences between NAC and RAC beams loaded at 7 days and slightly larger values for RAC loaded at 28 days compared with its reference NAC. Additionally, the RAC beams had smaller crack spacings and crack widths than reference NAC beams.

*Figure 12 – NAC and RAC beams in the laboratory*

## 3.2. Analytical research

Beside experimental research, an extensive analytical work was based on meta-analysis of published experimental results compiled in comprehensive databases [33-35].

Tošić et al. [33] compiled a database of shrinkage results from 19 studies, comprising 125 shrinkage time curves with 424 data points. The authors first confirmed the suitability of the *fib* Model Code 2010 [36] shrinkage model's mathematical formulation for describing the time evolution of shrinkage, Figure 13a and whether differences in RAC and NAC shrinkage were attributable to horizontal or vertical scaling differences (i.e. are the differences only related to the magnitude of shrinkage or also to its time evolution) and found no indication of horizontal scaling [33]. Subsequently, the calculated versus experimental result comparison was performed for RAC and reference NAC shrinkage, Figure 13b. An overestimation of shrinkage by the *fib* Model Code 2010 shrinkage model was found both for NAC and RAC, however, a larger overestimation was found for RAC – these results are in agreement with those found by Silva et al. [30]. This difference could not be explained only by the differences in compressive strength and must therefore come from the differences in shrinkage [33].

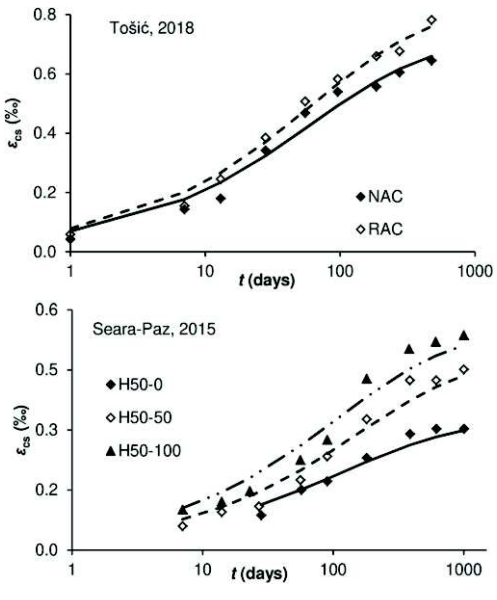


*Figure 13a – Calibration of individual shrinkage curves [33]*

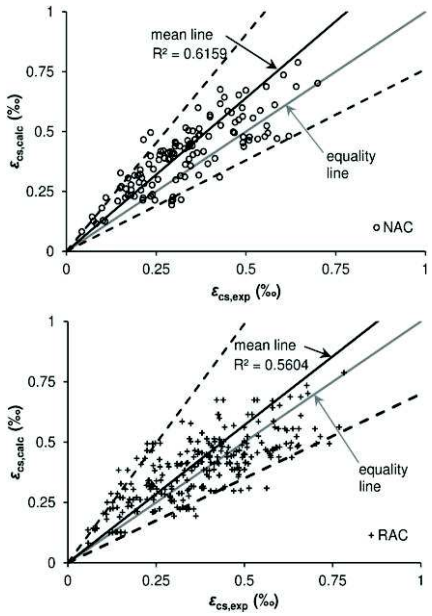


*Figure 13b – Calculated vs. experimental shrinkage strain values for NAC and RAC [33]*

Then, based on a regression that took into account bias in the time domain (by weighting data according to time decades), the authors proposed a global correction coefficient for RAC shrinkage:

$$\varepsilon_{\mathrm{cs,RAC}}(t,t_{\mathrm{s}}) = \xi_{\mathrm{cs,RAC}} \cdot \varepsilon_{\mathrm{cs}}(t,t_{\mathrm{s}}) = \left(\frac{RCA\%}{f_{\mathrm{cm}}}\right)^{0.30} \cdot \varepsilon_{\mathrm{cs}}(t,t_{\mathrm{s}}) \geq \varepsilon_{\mathrm{cs}}(t,t_{\mathrm{s}}) \quad (1)$$

where $\varepsilon_{\mathrm{cs,RAC}}(t,t_{\mathrm{s}})$ is the shrinkage strain of RAC cured until time $t_{\mathrm{s}}$ at time $t$, $\xi_{\mathrm{cs,RAC}}$ is the RAC shrinkage correction coefficient, *RCA%* is the mass percentage of coarse RCA in RAC, $f_{\mathrm{cm}}$ is the RAC compressive strength and $\varepsilon_{\mathrm{cs}}(t,t_{\mathrm{s}})$ is the shrinkage strain calculated according to the *fib* Model Code 2010 as for NAC. As can be seen, the model has the benefit of using only data known at the design stage – the compressive strength of RAC and the content of coarse RCA.

The similar procedure was followed by Tošić et al. [34] in analysing RAC creep. In this case, an experimental database from 10 studies was compiled, consisting of 46 creep time curves. Again, the authors used the *fib* Model Code 2010 [36] creep model and checked if differences in NAC and RAC creep are attributable to horizontal or vertical scaling (i.e. are the differences only related to the magnitude of creep or also to its time evolution). The authors converted all experimental data to creep coefficients according to the *fib* Model Code 2010 and analysed whether within individual time curves the ratio $\varphi_{\mathrm{MC,RAC}}/\varphi_{\mathrm{MC,NAC}}$ remained stable or changed over time. The authors found no indication of horizontal scaling of RAC creep [34].

Subsequently, the authors analysed predictions by the *fib* Model Code 2010 on the individual creep curves. The authors first confirmed the suitability of the model's mathematical formulation for describing the time evolution of creep and then the calculated versus experimental result comparison was performed for RAC and reference NAC creep whereby clear underestimation of RAC creep relative to reference NAC was observed. Finally, based on a regression that took into account bias in the time domain (by weighting data according to time decades), the authors propose a global correction coefficient for RAC creep:

$$\varphi_{\mathrm{RAC}}(t,t_0) = \xi_{\mathrm{cc,RAC}} \cdot \varphi(t,t_0) = 1.12 \cdot \left(\frac{RCA\%}{f_{\mathrm{cm}}}\right)^{0.15} \cdot \varphi(t,t_0) \geq \varphi(t,t_0) \quad (2)$$

where $\varphi_{\mathrm{RAC}}(t,t_0)$ is the creep coefficient at time $t$ of RAC loaded at time $t_0$, $\xi_{\mathrm{cc,RAC}}$ is the RAC creep correction coefficient, *RCA%* is the mass percentage of coarse RCA in RAC, $f_{\mathrm{cm}}$ is the RAC

compressive strength and $\varphi(t,t_0)$ is the creep coefficient calculated according to the *fib* Model Code 2010 as for NAC. As for the case of shrinkage, the model has the benefit of using only data known at the design stage – the compressive strength of RAC and the content of coarse RCA.

Finally, with regards to modelling deflection behavior of RAC structures, Tošić et al. [35] proposed a modification to the *fib* Model Code 2010 $\zeta$–method of deflection or curvature interpolation between the cracked and uncracked states. The authors considered the general form of the $\zeta$-method based on curvatures (where curvatures can be changed directly for deflections $a$):

$$\left(\frac{1}{r}\right)_{eff} = \zeta \cdot \left(\frac{1}{r}\right)_2 + (1-\zeta) \cdot \left(\frac{1}{r}\right)_1 \tag{3}$$

where $(1/r)_{eff}$ is the effective/interpolated curvature, while $(1/r)_1$ and $(1/r)_2$ are curvatures in the uncracked and fully cracked states, respectively, and $\zeta$ is a distribution coefficient taking into account tension stiffening:

$$\zeta = \begin{cases} 1-\beta \cdot \left(\frac{M_{cr}}{M}\right)^2 & \text{for } M \geq \sqrt{\beta} \cdot M_{cr} \\ 0 & \text{for } M < \sqrt{\beta} \cdot M_{cr} \end{cases} \tag{4}$$

where $\beta$ is a coefficient accounting for the influence of the duration of loading or repeated loading.

$$\begin{gathered} \beta = 1.0 \quad \text{for single, short} - \text{term loading} \\ \beta = 0.5 \quad \text{for sustained or repeated loading} \end{gathered} \tag{5}$$

The authors calibrated the model against experimental results from three studies [30,37,38] which comprised a database of 10 NAC and 15 RAC beams providing 20 and 30 deflections, respectively (initial and "final reported" time-dependent deflection). The range of parameter values in the database is presented in Table 1.

*Table 1 – Range of parameters in the NAC and RAC beam database [35]*

| ***Beams*** | ***RCA*** **(%)** | ***b*** **(mm)** | ***d*** **(mm)** | $f_{cm}$ **(MPa)** | ***L*** **(mm)** | ***L/d*** **(–)** | $\rho_1$ **(%)** | $t_0$ **(d)** | ***t*** **(d)** | $M_{sus}/M_{cr}$ **(–)** |
|---|---|---|---|---|---|---|---|---|---|---|
| NAC | 0 | 150–200 | 169–249 | 30.5–60.7 | 3200–3700 | 13.7–18.9 | 0.58–1.32 | 7–42 | 119–1000 | 0.81–3.35 |
| RAC | 50, 100 | | | 28.1–51.8 | | | | | | 0.68–2.52 |

The authors calculated deflections for the beams in the database using *fib* Model Code 2010 predictions for all properties, based on compressive strength and detected an underestimation of RAC deflections by the model, relative to NAC beams, especially for time-dependent deflections. Therefore, the authors attempted to identify whether the differences originated from the misestimation of RAC modulus of elasticity, shrinkage and creep (i.e. only from the material level) or also from a difference in tension stiffening (structural level). After implementing the changes for creep and shrinkage predictions based on Equations (1) and (2), respectively, and a reduction of the modulus of elasticity by (1 – 0.3*RCA%*/100), the authors still detected an underestimation of RAC deflections. Therefore, it was concluded that changes to tension stiffening modelling were also necessary. Hence, the following change to the $\beta$ coefficient was proposed:

$$\begin{gathered} \beta_{0,\mathrm{RAC}} = 0.75 \quad \text{for single, short} - \text{term loading} \\ \beta_{t,\mathrm{RAC}} = 0.25 \quad \text{for sustained or repeated loading} \end{gathered} \tag{6}$$

# 4. FLY ASH CONCRETE – PROPERTIES AND STRUCTURAL BEHAVIOUR OF BEAMS UNDER SHORT-TERM LOADING

Decarbonatization of concrete is, in a big part, focused on the use of supplementary cementitious materials (SCMs) to reduce the amount of Portland cement. A variety of SCMs are being used in concrete worldwide, and available quantities are reducing. In Serbia, a great amount of fly ash (FA), by-product obtained from coal combustion in thermal power plants, are available (Figure 14 left). Since 2010, Serbian fly ash is classified as non-hazardous waste that can be used as a secondary raw material. Therefore, a systematic analysis of the possibility to use high amounts of fly ash as a partial replacement of cement has been conducted at the Faculty of Civil Engineering in Belgrade. First, evaluation of high-volume fly ash concrete, HVFAC (Figure 14 right) made with more than 50% of fly ash was conducted. The analysis included experimental testing of physical and mechanical properties of HVFAC and testing of short-term behaviour of beams made with that concrete. Second, the reduction of cement was taken to a new level with the preliminary analysis of alkali-activated concretes made with total replacement of cement with fly ash.

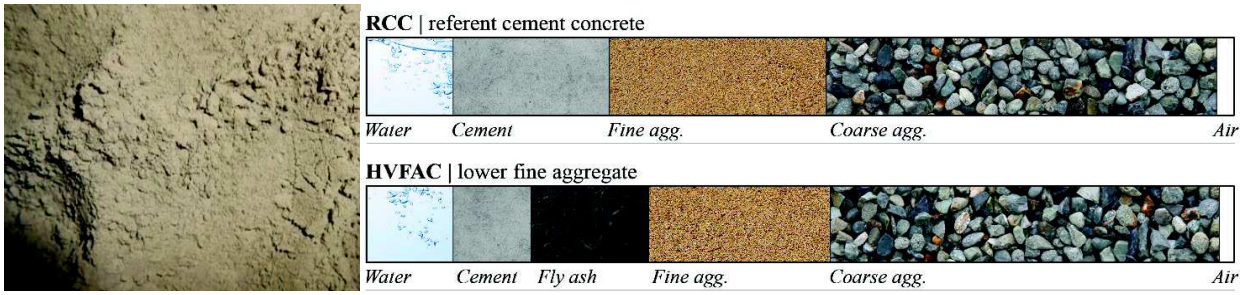


*Figure 14 – Fly ash (left), and high-volume fly ash concrete (right)*

## 4.1. High-volume fly ash concrete

### *4.1.1. Material properties*

A first step in this research was the development of HVFAC mixtures with fly ash from „Nikola Tesla B“ power plant in Serbia. The main objective here was to produce a HVFAC mix with the maximum possible fly ash amount that could yield a structural grade concrete. For that purpose, target strengths of 30 MPa after 28 days, and 20 MPa after seven days were selected. Ten concrete mixtures were made to get a better understanding of the effect of cement and fly ash amount on the physical and mechanical properties of HVFAC.

FA is a by-product that belongs to the class of Naturally Occurring Radioactive Materials (NORM), and therefore, the utilization of fly ash in concrete should be also considered from a radiological point of view. The natural radionuclide content of inbuilt building materials can have an effect on human health which can be different from the outdoor value. In 2013/59/Euratom Directive and in many other national standards regulating the radioactivity of building materials, classification is based on activity concentration index (I-index), considering the total effect of three main natural radionuclides usually present in building materials – $^{226}$Ra, $^{232}$Th and $^{40}$K. Therefore, radiological analysis of all ten mixtures is conducted and evaluated using the I-index.

Fly ash used for the preparation of HVFAC mixtures corresponded to ASTM C 618 [39] class F, with average mean particle size of 8.53 μm. Specific gravity was determined according to EN 450-1 [40] as 2075 kg/m$^3$. All concrete mixtures were made with commercially available blended Portland cement CEM II/A-M (S-L) 42.5R. In order to improve the workability of concrete, a polycarboxylate ether polymer-based superplasticizer (Glenium ACE, *BASF d.o.o.*) was used in some mixtures. River sand and coarse river aggregate with a 16 mm nominal maximum size were used.

Table 2 shows two groups of concrete mixtures made with different amounts of cement, 200 and 150 kg/m$^3$ and fly ash amount ranging from 50% to 70% of total SCMs mass.

*Table 2 – HVFAC mix design*

| Concrete mix | FA/CM | W/CM | W | C | FA | Sand | Coarse | SP |
|---|---|---|---|---|---|---|---|---|
| | % | - | kg/m$^3$ | | | | | |
| *C200F200_049* | 50 | 0.49 | 195 | 200 | 200 | 811 | 810 | 0.0 |
| *C200F250_043* | 55 | 0.43 | 195 | 200 | 250 | 749 | 810 | 1.0 |
| *C200F300_039* | 60 | 0.39 | 195 | 200 | 300 | 687 | 810 | 1.2 |
| *C200F350_036* | 64 | 0.36 | 195 | 200 | 350 | 625 | 810 | 2.2 |
| *C200F400_033* | 67 | 0.33 | 195 | 200 | 400 | 563 | 810 | 2.4 |
| *C150F150_061* | 50 | 0.61 | 183 | 150 | 150 | 879 | 878 | 0.0 |
| *C150F200_052* | 57 | 0.52 | 183 | 150 | 200 | 817 | 878 | 0.0 |
| *C150F250_046* | 63 | 0.46 | 183 | 150 | 250 | 755 | 878 | 0.0 |
| *C150F300_041* | 67 | 0.41 | 183 | 150 | 300 | 693 | 878 | 0.3 |
| *C150F350_037* | 70 | 0.37 | 183 | 150 | 350 | 631 | 878 | 1.1 |

CM – cementitious material (cement and FA); W – water; SP – superplasticizer.

Workability was determined using the slump test (Abrams cone), and for concrete mixtures that had higher slump values than 220 mm, flow table tests were performed. More details about this experimental research are shown in [41], and only basic mechanical properties (compressive strength, splitting tensile strength and modulus of elasticity) are shown in Table 3. Comprehensive radiological analysis of component material and all concrete mixtures is shown [42], and only I-index values for ten HVFAC mixtures are shown Table 3.

*Table 3 – HVFAC testing results*

| Concrete mix | Slump/ Flow (cm) | Compressive strength (MPa) | | | Splitt. tens. strength (MPa) | Modulus of elasticity (GPa) | | I-index |
|---|---|---|---|---|---|---|---|---|
| Age (days) | 0 | 7 | 28 | 90 | 28 | 28 | 90 | 0.28 |
| *C200F200_049* | 12.7 | 22.7 | 34.2 | 44.2 | 2.9 | 31.3 | 34.8 | 0.29 |
| *C200F250_043* | 14.8 | 22.9 | 38.2 | 42.3 | 2.7 | 32.1 | 33.7 | 0.29 |
| *C200F300_039* | 2.8 | 22.2 | 36.7 | 42.8 | 2.9 | 31.8 | 32.5 | 0.33 |
| *C200F350_036* | 3.3 | 27.1 | 42.0 | 47.9 | 3.7 | 33.2 | 35.1 | 0.32 |
| *C200F400_033* | 70.0* | 23.3 | 40.2 | 54.2 | 2.0 | 32.7 | 33.3 | 0.23 |
| *C150F150_061* | 8.2 | 12.9 | 24.3 | 28.5 | 2.5 | 29.0 | 35.5 | 0.26 |
| *C150F200_052* | 5.8 | 15.6 | 25.7 | 32.8 | 2.3 | 31.9 | 34.6 | 0.29 |
| *C150F250_046* | 8.3 | 14.2 | 24.5 | 33.8 | 3.1 | 30.0 | 32.6 | 0.33 |
| *C150F300_041* | 4.0 | 16.1 | 26.8 | 38.0 | 2.9 | 30.1 | 30.2 | 0.33 |
| *C150F350_037* | 58.5* | 16.0 | 29.8 | 39.3 | 3.2 | 30.2 | 33.1 | 0.28 |

*flow values

As can be seen from presented workability test results, with increasing the fly ash content, concrete mixtures became stiffer and those with more than 400 kg/m$^3$ of cementitious material (cement and FA) required the addition of superplasticizer in order to obtain a workable mix. Also, it was noticed that the content of superplasticizer should be increased with the increase of fly ash. However, no segregation and bleeding were noticed in any of the mixtures.

It is evident that the group of HVFAC mixtures made with 200 kg/m$^3$ of cement had higher compressive strength compared with the group made with 150 kg/m$^3$ of cement, for all fly ash contents and all ages. With the increase of fly ash content, compressive strength generally increased at all ages for both concrete groups, although the increase is rather low, maximally 20%. It is probably the consequence of a 'filler' effect of FA, resulting in a more compact structure of the concrete matrix. As can be seen, all concrete mixtures from the first group reached the target values defined as suitable for structural application of HVFAC (30 MPa after 28 days, and 20 MPa after seven days). Splitting tensile strength results indicate a large scatter and no reliable correlation with the fly ash content was found but, a similar relation between splitting tensile strength and compressive tensile

strength exist in HVFAC mixtures like in ordinary Portland cement concrete. The modulus of elasticity of HVFAC increased over time. When comparing HVFAC mixtures with the same fly ash content, in most cases higher moduli of elasticity were observed in concrete mixtures with greater cement content.

A comprehensive analysis of basic HVFAC mechanical properties was conducted based on own experimental results and the database of 440 HVFAC and 151 cement concrete mixtures collected from literature [43]. The analysis showed that the prediction models defined in EN 1992-1-1 for compressive strength, tensile strength and for modulus of elasticity can be used for HVFAC, in the given form or with modifications proposed in literature, with similar accuracy and variation of results as for cement concrete.

As can be seen in Table 3, the I-index for all HVFAC mixtures was significantly lower compared with the maximum defined level. The I-index value of 1 can be used as a conservative screening tool for identifying building materials that during their use would cause doses exceeding the reference level laid down in Article 75(1) of the 2013/59/EURATOM council directive. According to presented results, HVFACs made with up to 400 kg/m$^3$ of fly ash can widely be used as building materials, both for indoor or outdoor applications and for structural as well as for non-structural uses.

### *4.1.2. Structural behaviour*

Two HVFAC mixtures from the first phase of testing were selected for experimental research on beam elements. Flexural strength was tested on beams made with the C200F350_036 HVFAC mixture (C200F350 in further text) and shear strength on beams made with the C200F200_049 (C200F200 in further text) HVFAC mixture. Behaviour of beams was tested on a full-scale simply supported beam specimens (300 cm span) with rectangular cross-section (width of 20 cm and height of 30 cm) and a total length of 350 cm. A four-point bending test setup was used to compare the behaviour of HVFAC beams and Portland cement beams. Detailed experimental set up and the results are shown in [44].

To address the question of the HVFAC beams flexural behaviour, two groups of beams were made and tested. The first group was made with a minimum reinforcement ratio (3Ø8 tensioned longitudinal bars) and the second with a five times higher longitudinal reinforcement ratio (3Ø18 tensioned longitudinal bars). Two HVFAC (HVFAC-1 and HVFAC-2) and two referent cement beams (OPC-1 and OPC-2) with a targeted equal 90-day compressive strength were made and tested. The geometry and properties of corresponding HVFAC and cement beams along with the experimental set-up were designed to be identical, differing only in the concrete type. All beams were equipped for continuous measurement of applied force; deflection in five points along beams length; concrete strains in three cross sections; longitudinal reinforcement strains and crack widths.

All beams were tested until failure and presented similar behaviour in all steps until failure (Figure 15 and Figure 16). The crack propagation in the beams began with the appearance of flexural cracks in the maximum moment region. The first flexural cracks appeared at lower loading levels for HVFAC beams compared with the cement beams: 25% lower for beams with a minimum reinforcement ratio and 16% lower for beams with a higher reinforcement ratio. Before the first flexural crack formation, all of the beams showed similar linear–elastic behaviour. After the additional load was applied, the longitudinal steel yielded. With further load increase, compressed concrete crushed and the beams failed. In the beams with the minimum longitudinal reinforcement ratio, failure occurred after the crushing of concrete and braking of the longitudinal reinforcement. The difference between the cement beams and HVFAC ultimate loading levels was not significant.

The comparative analysis of the longitudinal reinforcement strains in the HVFAC and cement beams showed no significant difference between the load–strain curves of different concrete beams prior to

flexural cracking. The concrete compressive strains at failure were higher in HVFAC beams compared with the cement beams, but the difference was only up to 9% for all measured sections.

a)

b)

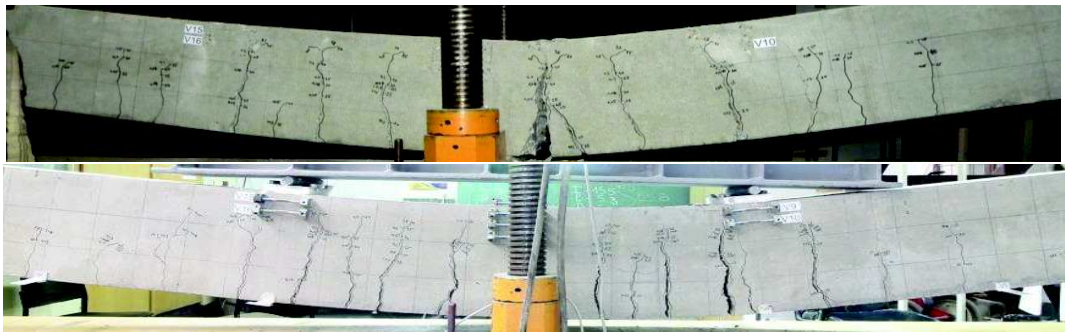

*Figure 15 – Failure of beams tested under bending a) OPC-1, b) HVFAC-1*

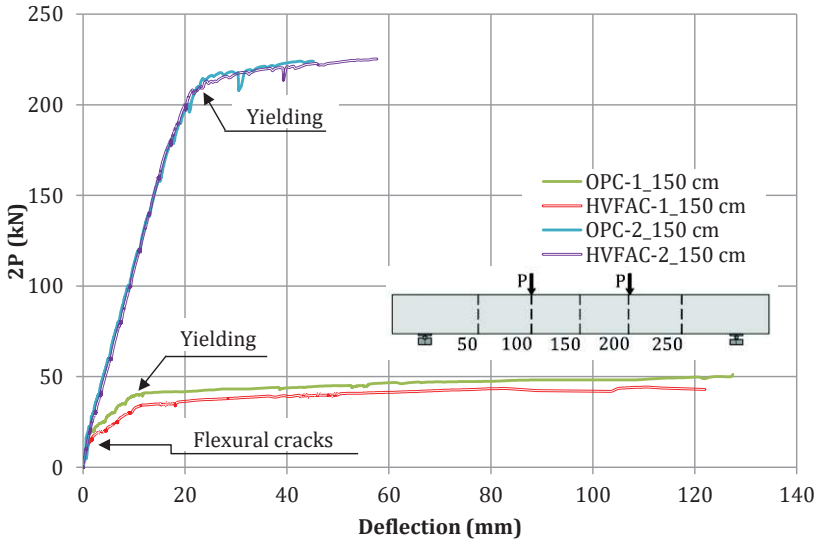


*Figure 16 – Load-deflection curves for all beams tested under bending*

The maximum deflections of HVFAC beams at the service load level were higher compared with the cement beams, especially in the beams with a minimum reinforcement ratio. This difference decreased as the ultimate loading level approached. The analysis of load-deflection curves showed that the stiffness of the tested HVFAC beam with a minimum reinforcement ratio was lower than the stiffness of the cement beam, differing by not more than 11%. This difference was relatively small in beams with a higher than minimum reinforcement ratio.

The first flexural crakes appeared at 25% and 33% lower loading level for HVFAC-1 and HVFAC-2 beams compared with the corresponding cement beams. A higher number of flexural cracks, higher crack lengths and widths, and more cracks branching developed in HVFAC beams compared with the corresponding cement beams. These effects were more pronounced in the beams with the minimum longitudinal reinforcement ratio.

Comprehensive analysis of the possibility to apply existing code provisions (BAB ’87, EN 1992-1-1, and ACI 318) on the flexural strength prediction calculation shows that the available code provisions for the cement members can be applied for the ultimate bending moment prediction of HVFAC members with equal accuracy.

Similar methodology was applied for testing shear behaviour of beams. To address the concern of the shear strength of HVFAC beams compared with the cement beams, full-scale shear tests were performed on six beams. All beams in this part of the study had the same longitudinal reinforcement and different shear reinforcement ratios. The first group of beams was made without shear reinforcement in the tested shear span (OPC-1 and HVFAC-1); the second group was made with a

minimum shear reinforcement ratio (OPC-2 and HVFAC-2); the third group of beams was made with twice the minimum shear reinforcement (OPC-3 and HVFAC-3). Results of the first and second groups of beams are briefly described in the following text.

The difference between the cement beams and HVFAC beams ultimate shear stress levels was not significant (Figure 17). In beams without shear reinforcement, the crack progression began with flexural cracks occurring in the beams' maximum moment region close to the location of applied load points. As the load increased, the number of flexural cracks increased in the middle part of the beam and in the shear span. At a point of approximately 75% of the ultimate load short diagonal shear crack began to appear in the middle part of the shear region. Failure of both cement and HVFAC beams occurred in a brittle manner when the diagonal crack reached the loading point (Figure 18). Both cement and HVFAC beam specimens exhibited linear-elastic behaviour approximately until the formation of the diagonal crack. The behaviour of beams with shear reinforcement was similar to the behaviour of beams without stirrups up to the point of first shear crack formation at 50-60% of the ultimate shear load. All beams with shear reinforcement showed a significant bearing capacity after diagonal crack formation until failure. The difference between cement and HVFAC beams falls within a 10% margin.

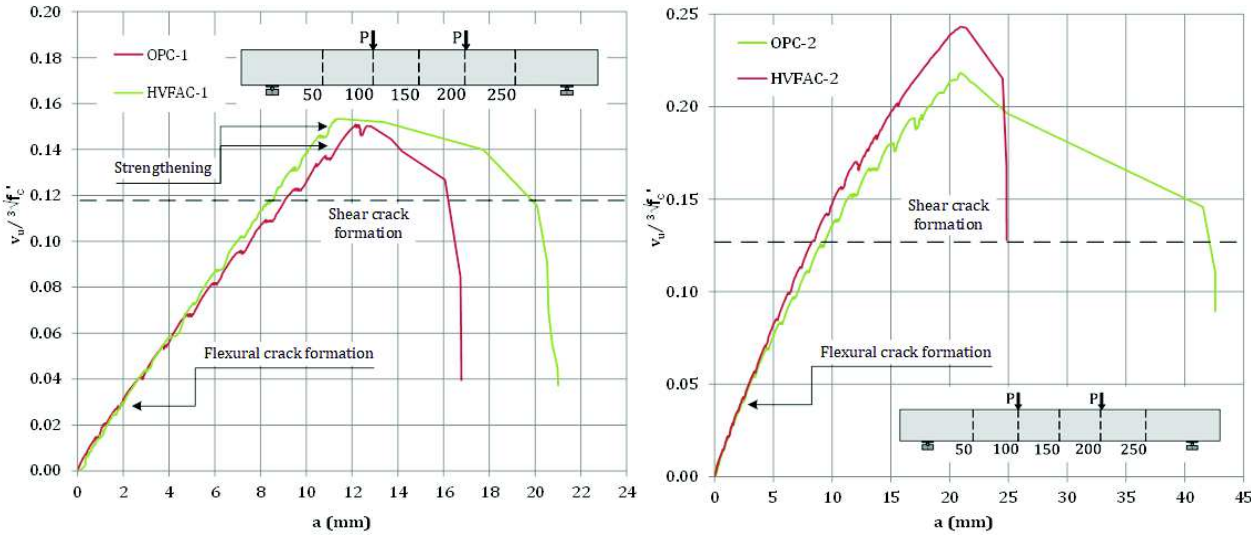


*Figure 17 –Load-deflection curves for beams without shear reinforcement (left) and beams with shear reinforcement (right)*

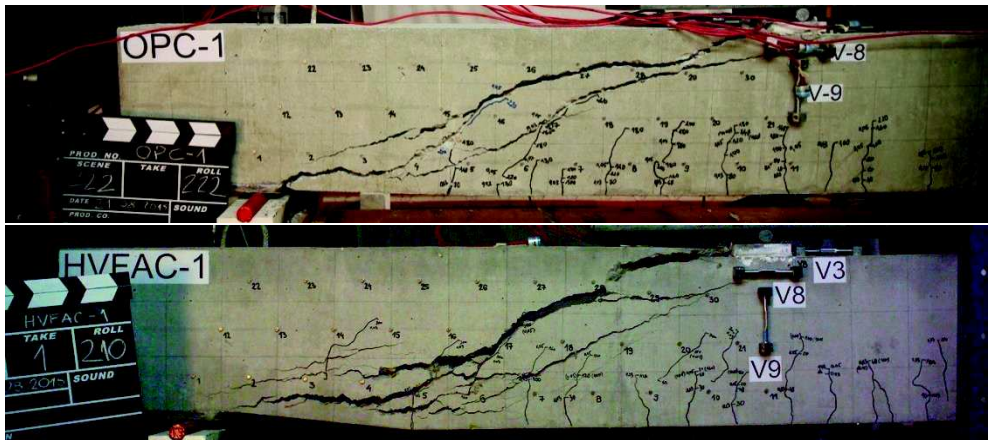


*Figure 18 – Failure of beams without shear reinforcement a) OPC-1, b) HVFAC-1*

Reinforcement strains developed in the same way for both OPC-1 and HVFAC-1 beams without shear reinforcement until the first flexural cracks appeared. After that point in all three sections, the OPC-1 beam had higher strains for the same normalized shear stress. The maximum strain values

in each measured section showed that the difference between the OPC-1 and HVFAC-1 beams was in the 10% margin. Reinforcement strains developed in the same way for beams with shear reinforcement until flexural cracks appeared. After that point, the OPC beams had higher strains for the same normalized shear stress with the difference being within the 20% margin. A general trend is showing higher stirrups strains in the HVFAC beams compared with the OPC ones.

Concrete compressive strains at failure were higher in OPC beams compared with the HVFAC ones. The ultimate concrete strains ranged from 2.68‰ to 3.98‰. The concrete compressive strains were, on average, 12% and 19% higher in the OPC-1 and OPC-2 beams compared with the corresponding HVFAC beams, respectively. It was noticed that the distribution of strains along the beam's height was linear with practically the same compressed concrete zone height in all beams which failed in shear.

The maximum deflection under service loading was not significantly different in cement and HVFAC beams. The inclination of the linear-elastic part of the deflection-stress relationship was up to 10% higher for all HVFAC beams compared with the cement ones.

The application of EN 1992-1-1, ACI 318, and fib Model Code 2010 on the shear strength prediction calculation shows no significant difference between the cement and HVFAC beams. The difference is only up to 6%.

## 4.2. Alkali-activated concrete

Alkali-activated concrete is a trending type of concrete and the idea to alkali activate (AA) local pozzolanic material and produce concrete binder was also tackled during one experimental program conducted at the Faculty of Civil Engineering in Belgrade. In this study, the potential use of class F fly ash from thermal power plant „Nikola Tesla B" as an alkali activated binder in concrete composites was studied. The experimental program was designed to investigate the influence of various parameters on the concrete compressive strength and workability.

For the activator, a combination of sodium silicate ($Na_2SiO_3$) and sodium hydroxide (NaOH) was chosen. Sodium silicate solution $Na_2O{\cdot}n{\cdot}SiO_2$ had a module of n=1.91 and a specific gravity of 1514 kg/m$^3$. The NaOH used in the study was technical grade with 98% purity, in pellets. In this study two samples of fly ash (FA-3 and FA4) were taken from the two finest fractions. The average mean particle size is 16.775 μm for FA-3 and 8.533 μm for FA-4.

First, alkali activated fly ash pastes (AAFAP) were produced with different alkali activator combinations in order to investigate their effect on the compressive strength and workability. The aim was to find the best possible binder for later use in AAFAC. To achieve this, the effect of different activator combinations on the two fly ashes was studied. The properties of the activator solutions along with mixture proportions are presented in Table 4.

To accelerate the reaction, process all specimens were cured at 80ºC. This temperature was chosen as usual for accelerated curing of concrete and as suitable for the geopolymerization of fly ash. To test the speed of the reaction, specimens were cured for 6 and 24 h. Once the elevated heating was completed, all the specimens were stored at standard laboratory conditions until testing at 48 h after mixing.

The results showed that better workability and compressive strength can be achieved with FA-4, and that the curing time did have a significant influence on the behaviour of AAFAP. Also, increase in compressive strength both for rising molarity of NaOH and for the rising $Na_2SiO_3$/NaOH ratio was noticed. Because of this, analysis of AAFAC was conducted with FA-4 and a curing time of 6 h.
All of the AAFAC mixtures were again designed with 400 kg/m$^3$ of FA and an AA/FA ratio of 0.6. Aggregate with maximum size of 16 mm was used in saturated surface dry condition. All samples were cast in 10-cm cubes, vibrated and sealed with a layer of plastic sheet. According to the results

of AAFAPs, the specimens were cured for only 6 h at a temperature of 80ºC. After curing, all the specimens were stored at standard laboratory conditions until testing at 1, 3, 7 and 28 days after mixing.

*Table 4 – Mixture proportions and compressive strength - fp of AAFAP*

| | AA/FA | NaOH | $Na_2SiO_3$ /NaOH | $Na_2O$/ FA | $SiO_2$/ $Na_2O$ | $H_2O$/SOL* | $f_p$/6 h | $f_p$ /24 h |
|---|---|---|---|---|---|---|---|---|
| | (–) | (M) | (–) | (%) | (–) | (–) | (MPa) | (MPa) |
| **A3.1** | 0.6 | 10 | 2.0 | 10.72 | 1.04 | 0.312 | 40.78 | 44.53 |
| **A3.2** | 0.6 | | 3.5 | 10.09 | 1.30 | 0.299 | 47.66 | 45.63 |
| **A3.3** | 0.6 | | 5.0 | 9.77 | 1.44 | 0.292 | 45.00 | 48.00 |
| **A3.4** | 0.6 | | 10.0 | 9.34 | 1.64 | 0.284 | 45.31 | 46.96 |
| **A3.5** | 0.6 | 16 | 2.0 | 12.86 | 0.87 | 0.290 | 42.00 | 48.00 |
| **A3.6** | 0.6 | | 3.5 | 11.51 | 1.14 | 0.284 | 48.75 | 48.59 |
| **A3.7** | 0.6 | | 5.0 | 10.84 | 1.30 | 0.282 | 45.94 | 48.13 |
| **A3.8** | 0.6 | | 10.0 | 9.92 | 1.54 | 0.278 | 50.94 | 55.16 |
| **A4.1** | 0.6 | 10 | 2.0 | 10.72 | 1.04 | 0.312 | 57.11 | 54.30 |
| **A4.2** | 0.6 | | 3.5 | 10.09 | 1.30 | 0.299 | 49.22 | 53.91 |
| **A4.3** | 0.6 | | 5.0 | 9.77 | 1.44 | 0.292 | 55.31 | 56.88 |
| **A4.4** | 0.6 | | 10.0 | 9.34 | 1.64 | 0.284 | 59.69 | 56.95 |
| **A4.5** | 0.6 | 16 | 2.0 | 12.86 | 0.87 | 0.290 | – | – |
| **A4.6** | 0.6 | | 3.5 | 11.51 | 1.14 | 0.284 | 53.91 | 60.16 |
| **A4.7** | 0.6 | | 5.0 | 10.84 | 1.30 | 0.282 | 58.83 | 59.92 |
| **A4.8** | 0.6 | | 10.0 | 9.92 | 1.54 | 0.278 | 65.42 | 75.63 |

*$H_2O$/SOL- the mass ratio of total water to fly ash, $Na_2O$ and $SiO_2$ (contained in $Na_2SiO_3$ and NaOH)

As for the activator, it was decided not to vary specific molarities of NaOH or specific $Na_2SiO_3$/NaOH ratios but rather to design activator solutions for discrete values of $Na_2O$/FA and $SiO_2/Na_2O$ ratios ratios since the geopolymerization process in fact depends on them.Eight mixtures were designed for 2 different $Na_2O$/FA ratios and 5 different $SiO_2/Na_2O$ ratios (Table 5).

*Table 5 – Mixture proportions of AAFAC*

| Specimen | NaOH | $Na_2SiO_3$ | Coarse aggr. | Fine aggr. | $Na_2O$/ FA | $SiO_2$/ $Na_2O$ |
|---|---|---|---|---|---|---|
| | (kg/m$^3$) | (kg/m$^3$) | (kg/m$^3$) | (kg/m$^3$) | (%) | (–) |
| **C1** | 60.19 | 179.81 | 992.3 | 661.5 | 9.35 | 1.35 |
| **C2** | 46.87 | 193.13 | 993.2 | 662.1 | 9.35 | 1.45 |
| **C3** | 33.55 | 206.45 | 989.3 | 659.5 | 9.35 | 1.55 |
| **C4** | 20.24 | 219.76 | 989.9 | 659.9 | 9.35 | 1.65 |
| **C5** | 63.71 | 176.28 | 992.0 | 661.4 | 9.90 | 1.25 |
| **C6** | 49.62 | 190.38 | 993.0 | 662.0 | 9.90 | 1.35 |
| **C7** | 35.51 | 204.49 | 994.0 | 662.6 | 9.90 | 1.45 |
| **C8** | 21.41 | 218.59 | 986.3 | 657.5 | 9.90 | 1.55 |

The increase in compressive strength from day 1 to 28 ranges from 3% to 27% with an average value of 17% (Figure 19). Decrease of compressive strength over time was noticed in some AAFAC mixtures. This is most likely a consequence of different samples used for measuring each strength and the fact that heat curing accelerated strength development, so traditional trend cannot be expected here. For each $SiO_2/Na_2O$ ratio, higher compressive strengths are achieved for the concretes with a higher $Na_2O$/FA ratio. These results point to a fact that there is an optimal $SiO_2/Na_2O$

ratio, not necessarily the highest one. For both values of $Na_2O$/FA ratio, the highest concrete compressive strengths at 28 days were obtained for $SiO_2/Na_2O$ ratio equal to 1.45.

Radiological properties of AAFAC were also tested. The results [45] showed that I-index values are significantly lower than the upper value, and that this type of concrete can be safely used.

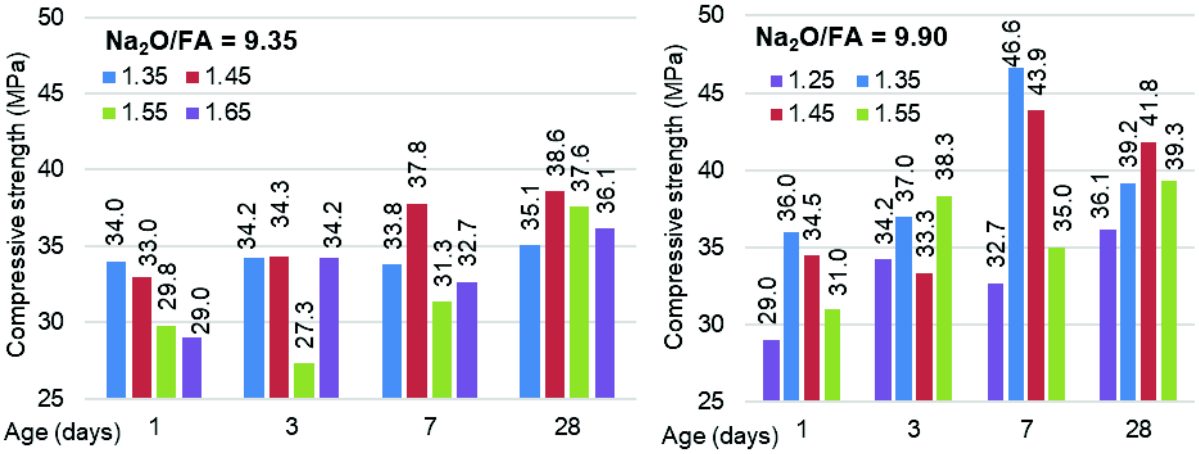


*Figure 19 – Development of compressive strength for mixtures with different SiO2/Na2O ratios*

It can be concluded that FA-4 from “Nikola Tesla B” can be used as a component material for structural AAFAC production. However, this type of concrete requries curing at elevated temperatures and it can be used only in precast concrete applications.

## 5. DURABILITY OF RECYCLED AGGREGATE AND FLY ASH CONCRETES

The use of RCA or FA for the production of new concrete greatly affects the physical and mechanical properties of concrete. In order to ensure the sustainable application of these green alternatives, the durability properties of RAC and HVFAC should also be tested. The durability of concrete is defined by its resistance to the action of harmful agents from the external environment that lead to various types of damage (deterioration mechanisms). Deterioration mechanisms can affect the concrete structure (freeze/thaw with or without de-icing agents, alkali-silicate reaction and sulphate action) or can cause reinforcement corrosion (carbonation and chloride penetration). Although concrete was considered as a material with good durability properties, cases of insufficient service life are not uncommon [46]. The main reason for the deterioration of reinforced concrete (RC) structures is the corrosion of steel reinforcement [47]. Carbonation-induced corrosion has been reported as a major durability problem in urban conditions, considering a large number of buildings that are exposed to a $CO_2$-rich environment [48]. In this regard, research focused on RAC and HVFAC carbonation resistance was conducted.

### 5.1. Carbonation resistance of different concrete types

An experimental programme was carried out from 2017 to 2020, at the Faculty of Civil Engineering, University of Belgrade. For the purpose of this research, three concrete mixtures were prepared and tested: reference ordinary Portland cement concrete with NA (*NAC*), concrete with 100% replacement of coarse NA with RCA (*RAC*) and concrete with 50% of class F FA in total cementitious materials mass (*HVFAC*). The RCA had an oven-dry density of 2370 kg/m$^3$ and water absorption of 3.9% after 24 hours. FA used in this study was a by-product from the coal combustion in thermal power plant "Nikola Tesla B" in Obrenovac, Serbia, and its specific gravity was 2075 kg/m$^3$, and the mean particle size was 8.53 μm. All mixtures were prepared with similar compressive strengths (41.0, 41.7 and 42.1 MPa, respectively) and same workability class (S3). The analysis was carried out using own experimental results and the application of available standards and novel predictions regarding carbonation depth.

At the beginning, a trial test of the optimal $CO_2$ concentration which will accelerate the carbonation process was performed (Figure 20a). Based on the conducted analysis, it has been shown that a $CO_2$ concentration up to 2% was optimal. In terms of material properties, approximately 40% and 115% higher carbonation depth was observed for RAC and HVFAC than for NAC respectively (Figure 20b), which is in line with previous literature reviews [49].

*Figure 20a – Samples in the carbonation chamber*

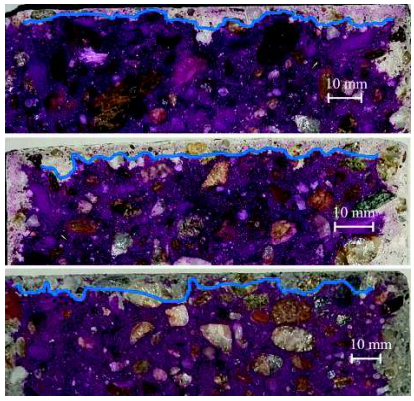


*Figure 20b – Carbonation depth over time for NAC, RAC and HVFAC, respectively*

Beside experimental research, an extensive analytical work was based on analysis of published experimental results compiled in comprehensive databases. Values of carbonation depth under accelerated conditions and corresponding compressive strength were found in 15 studies for NAC, 8 studies for RAC and 17 studies for fly ash concrete (FAC). A total of 115, 109, and 138 carbonation depth measurements were collected for NAC, RAC, and FAC, respectively. Based on the analysis it was concluded that the *fib* – Bulletin 34 [50] prediction model can be applied to all types of tested concretes, with modifications for FAC [47]. In order to achieve this, it is necessary to perform an accelerated carbonation test. Since this is not always possible, the relationship between carbonation resistance and design value of 28 days concrete's compressive strength ($f_{cm}$), which is most often used as an indicator of the concrete quality, was established [47,51]. This relationship is shown for RAC (Figure 21a) and for HVFAC (Figure 21b).

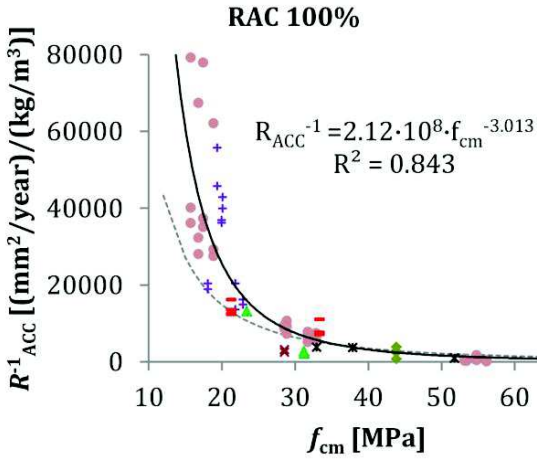


*Figure 21a – Relationship between carbonation resistance and $f_{cm}$ for RAC [47]*

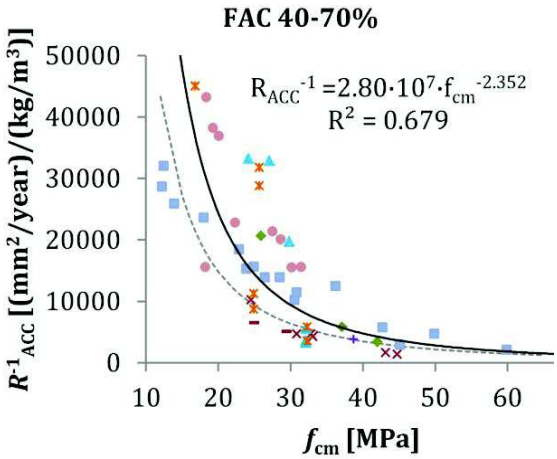


*Figure 21b – Relationship between carbonation resistance and $f_{cm}$ for HVFAC [47]*

Full probabilistic analysis of the service life of different concrete types was performed using accordingly modified *fib* – Bulletin 34 prediction model. The recommended values of minimum concrete cover depths for different concrete types are shown in Table 6.

*Table 6 – Values of minimum concrete cover depths for different types of concrete for $t_{SL}$ = 50 years [48]*

| **Type of concrete** | **$C_{min,dur}$ (mm)** | | | |
|---|---|---|---|---|
| | **XC1** | **XC2** | **XC3** | **XC4** |
| **Indicative strength class** | **C 25/30** | **C 25/30** | **C 30/37** | **C 30/37** |
| Referent concrete | 15 | 25 | 25 | 30 |
| RAC (10-50% replacement) | 15 | 25 | 25 | 30 |
| RAC (100% replacement) | 16 | 26 | 25 | 30 |
| FAC (10-35% of FA) | 22 | 35 | 40 | 39 |
| HVFAC (40-70% of FA) | 35 | 58 | 62 | 61 |

## 5.2. Influence of cracks on carbonation resistance

Deterioration processes and their transport mechanisms were studied and tested almost exclusively on uncracked concrete samples. Possibly the most important factor that affects the carbonation process is the appearance of cracks in RC structures. With relatively low tensile strength of concrete, the cracking of structural elements is almost inevitable due to different action effects. For that reason, the analysis of crack width on carbonation depth and prediction models was one of the main objectives of this research. Samples with different crack width (0.05 mm, 0.10 mm, 0.15 mm, 0.20 mm and 0.30 mm) and reference samples without cracks were made (Figure 22). All defined crack widths in this study were smaller than the acceptable crack widths defined in the European standard EN 1992-1-1 [27], – for given exposure condition the maximum crack width is defined as 0.3 mm.

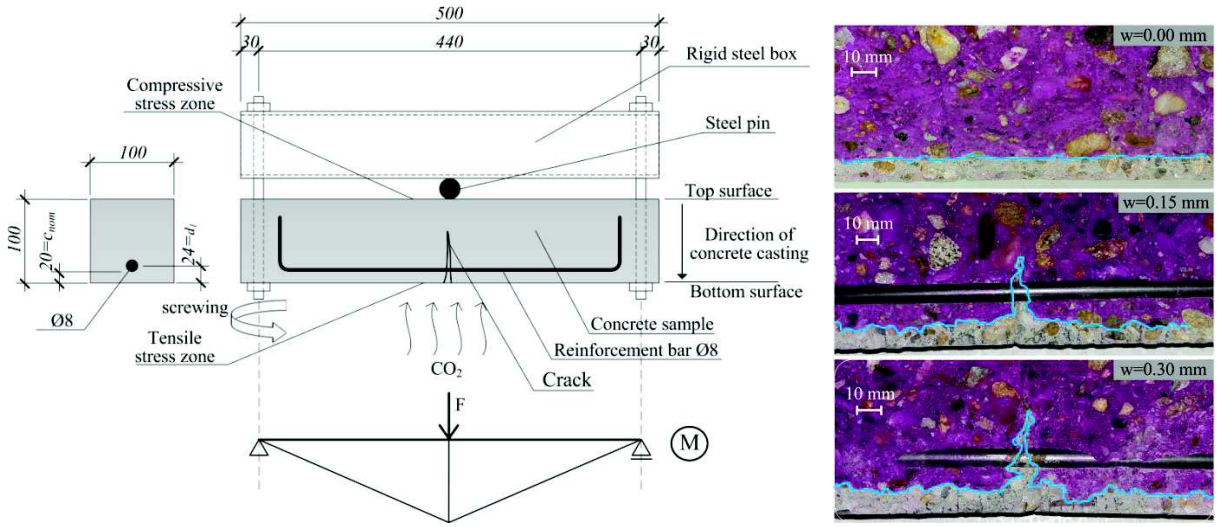


*Figure 22 – Experimental setup for testing the effect of cracks on concrete carbonation resistance [52]*

The analysis of cracks influence on carbonation induced corrosion was conducted using own experimental results and the application of available standards and novel predictions regarding carbonation depth. The influence of cracks on the carbonation front was approximately the same (20 mm) regardless of the crack width. In all cases, even for samples with smallest crack widths–0.05 mm, the cracks behaved as an additional exposed surface through which the $CO_2$ molecules were diffused perpendicularly to the crack wall. This phenomenon was the same for all samples, regardless of the concrete type [53]. Also, the carbonation depth of uncracked samples was up to three times lower compared to cracked samples. There was no significant difference between concrete types, indicating that the crack appearance had higher impact on carbonation depth compared with different concrete type as a parameter.

Surface crack width should not be an isolated parameter associated with reinforcement corrosion. It was shown that it is more useful to use the maximum reinforcement stress as a possible limitation

in terms of the influence of load-induced cracks on the development of reinforcement corrosion. In addition, the maximum stress in the reinforcement directly determines the damage of concrete at the reinforcement level. After the linear relationship between the carbonation depth and reinforcement stress level (Figure 23) for all types of tested concrete was established, the limit value of reinforcement stress was determined [48] (Figure 24). This was done by applying a semi-probabilistic model of corrosion prediction. Proposed procedure enables the service life calculation in terms of carbonation induced corrosion with higher reliability compared to reliability provided by exiting prediction models.

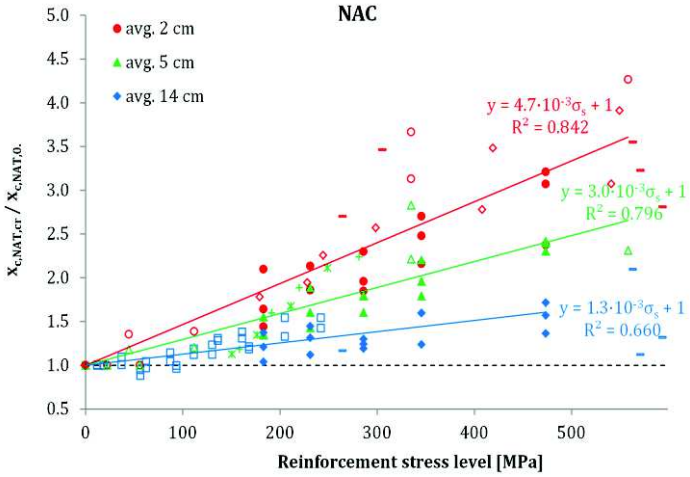


*Figure 23 – Relationship between carbonation depth and reinforcement stress for NAC [47]*

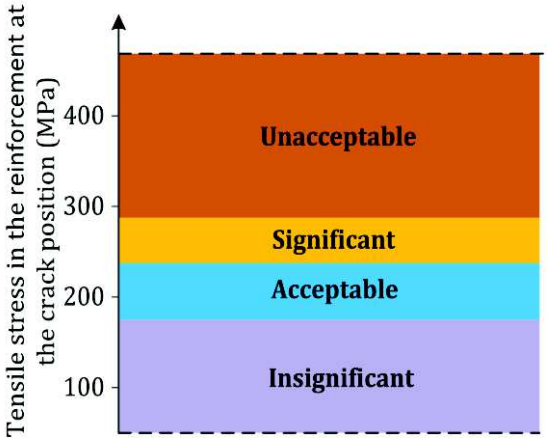


*Figure 24 – Relationship between reinforcement stress and damage level [47]*

## 6. SUSTAINABILITY ASSESSMENT

In order to introduce a new material or technology into the construction practice, its performance at all levels should be competitive to materials or technologies already existing on the market. Along with the experimental and analytical research on technical performance of various green solutions, their environmental performance was assessed using Life Cycle Assessment methodology [51,54-55].

One such assessment was performed with a goal to compare the environmental impact of the cradle-to-gate part of the life cycle of five different types of structural concrete [55]:

NAC – natural aggregate concrete made entirely with river aggregate and a cement binder
NAC_FA - natural aggregate concrete with 35% replacement of cement with fly ash
NAC_AAFA – alkali activated fly ash NAC
RAC – recycled aggregate concrete with natural fine and recycled coarse aggregate (100% replacement ratio) and a cement binder
RAC_FA - RAC with 35% replacement of cement with fly ash

All five concrete mixes were designed and experimentally verified to have the same compressive strength and workability. Functional unit in LCA included the impact of different deformational behaviour and carbonation resistance of alternatives. Possible lower carbonation resistance and higher long-term deflections in the course of 50 years of service life were taken into account by assuming that functional unit for NAC_FA, RAC and RAC_FA was equal to 1.1 $m^3$, while for other concrete types a functional unit equal to 1.0 $m^3$ was kept. Life cycle inventory data was taken for concrete production located in Serbia [56].

The calculated impact category indicators were: global warming potential (GWP), ozone layer depletion potential (ODP), eutrophication potential (EP), acidification potential (AP) and photochemical oxidant creation potential (POCP). They were calculated using the CML (The Institute

of Environmental Sciences of the Faculty of Sciences of Leiden University) baseline methodology [57]. Besides, abiotic depletion of fossil fuels potential (ADP_FF) was calculated using the cumulative energy demand method. However, indicators are expressed in different units and their absolute values vary significantly. In order to enable aggregation and calculation of a single sustainability indicator, normalization is performed using the Diaz-Balteiro [58] equation. This equation, in the case of a „less is better“ indicator type, can be formulated as:

$$\overline{I_i} = \frac{I_i - I_{i*}}{I_i^* - I_{i*}} \tag{7}$$

where $\bar{I}_i$ is the normalized value of *i*-th indicator, $I_{i*}$ and $I_i^*$ are the worst and the best value (minimum) of the *i*-th indicator, respectively. In this way, indicator's values are converted into dimensionless values ranging from 0 (worst value) to 1 (best value).

Normalized impact categories can be presented together in a 'radar' diagram showing in that way the so-called "sustainable profile". This type of presentation enables easier understanding of the complete environmental profile of the particular concrete, and for this specific case, it is shown in Figure 25 [55]. In this figure, the area of referent NAC profile and the area of NAC_AAFA profile are shaded. Then it can easily be seen that alkali activated concrete is better in GWP, AP and POCP, while non-alkali activated concretes are better in ADP_FF, ODP and EP.

Global sustainability indicator SI can be calculated by the aggregation of *n* normalized indicator's values:

$$SI = \sum_{i=1}^{n} w_i \overline{I_i} \tag{8}$$

where $w_i$ are the weights representing the relative importance of the *i*-th indicator for the overall environmental performance. The "most sustainable" product is then the product with the maximum SI value. The SI results for analyzed alternatives are presented in Table 7, if all six calculated indicators are equally important, i.e. the weight of each is equal to 1/6=0.1667.

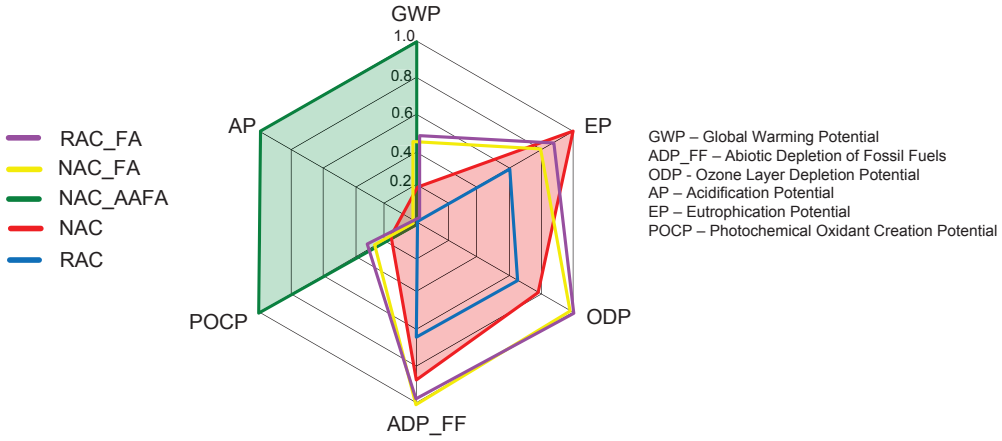


*Figure 25 – Normalized indicators in a 'radar' diagram for analyzed concrete alternatives [55]*

*Table 7 – Sustainability indicators for analyzed concrete alternatives [55]*

| Concrete type | RAC_FA | NAC_FA | NAC_AAFA | NAC | RAC |
|---|---|---|---|---|---|
| SI | 0.629 | 0.596 | 0.500 | 0.543 | 0.314 |

Based on this specific LCA, recycled aggregate concrete with a cement binder (RAC) showed the weakest overall environmental performance (the lowest SI), while RAC_FA showed the best performance. Hence, in order to achieve a better environmental performance of RAC, it should be designed with the same cement amount as NAC; the water-to-cement ratio should be decreased and workability problems solved with the aid of a superplasticizer.

Further in this line of investigation, Tošić et al. [59] used a multi-criteria decision-making method, VIKOR, to select for an optimal concrete mix for application in reinforced concrete columns. For this purpose, a case study was analyzed considering three concrete types:

NAC – natural aggregate concrete made entirely with river aggregate

RAC50 – recycled aggregate concrete with natural fine and 50% recycled coarse aggregate (with 50% being river gravel)

RAC100 – recycled aggregate concrete with natural fine and 100% recycled coarse aggregate

The concretes were real mix designs developed and verified in the lab for having comparable compressive strength and workability so that they could be used in the same structural application and with the same functional unit (1 $m^3$ of concrete).

For the analysis, local conditions for a construction site in Belgrade, Serbia, were considered in terms of material procurement and transport distances, Figure 26. The three alternatives were then evaluated according to five criteria: energy use, environmental load (considering an LCA analysis and GWP, EP, AP and POCP impact indicators), waste generation, mineral resource depletion and cost (cost of concrete constituent materials).

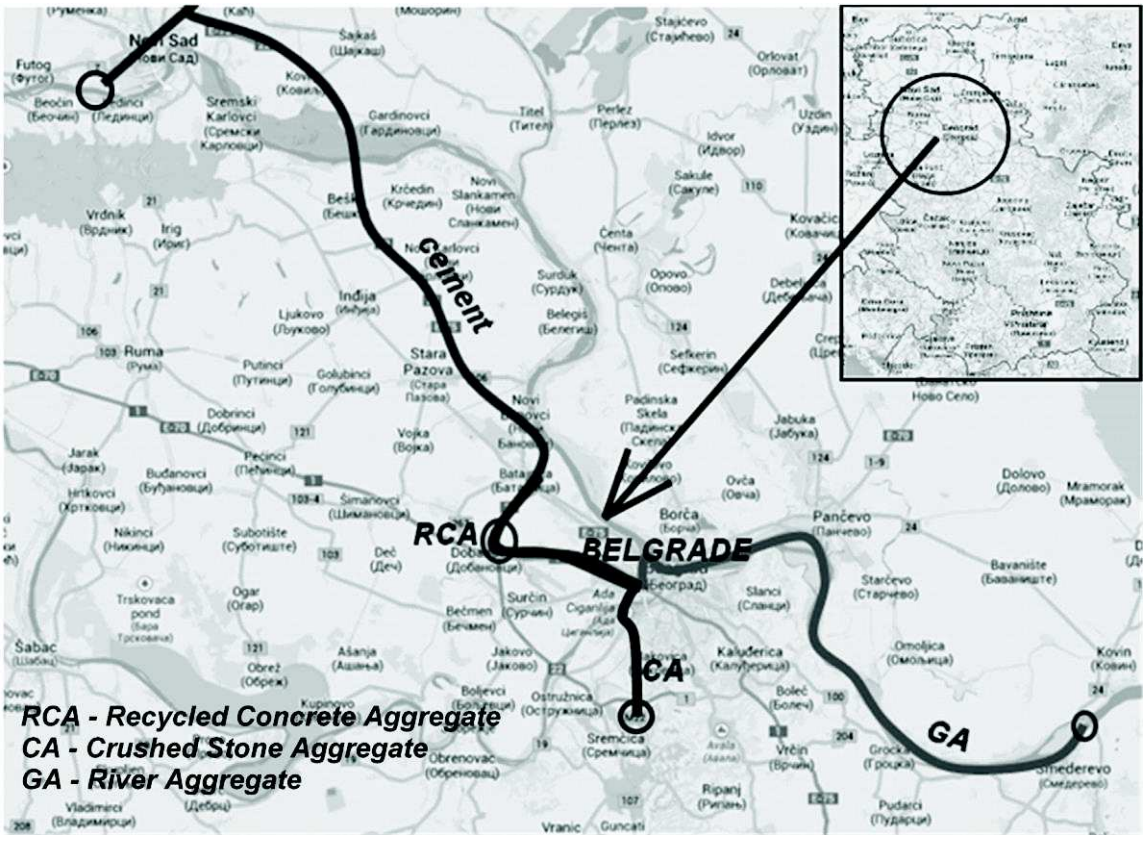


*Figure 26 – Transport scenarios for the case study in Belgrade, Serbia [59]*

In the VIKOR method, the value for each criterion and each alternative is evaluated considering the following metric:

$$L_{p,j} = \left\{ \sum_{i=1}^{n} \left[ w_i \left( f_i^* - f_{ij} \right) / \left( f_i^* - f_i^- \right) \right]^p \right\}^{1/p}, 1 \le p \le \infty; j = 1,2,\ldots J \quad (9)$$

where $L_{1,j}$ and $L_{\infty,j}$ are used to formulate the ranking or "closeness" measure (i.e. in Eq. (9) $p$ is 1 and ∞, respectively). The "distance" to the "ideal solution" is a distance in an n-dimensional space (n is the number of criteria) i.e. the difference between each criteria function value (for every alternative) and the "ideal" value is a component of a "distance" vector for each alternative.

After evaluating the alternatives, they are ranked considering a determined procedure and an adopted weighting of the criterions. In order to simulate the uncertainty of this step of the decision-making process, three criterion weightings were considered: equal importance (equal weights of all criteria), environmental preference (advantage given to the criteria related to environmental load, waste generation and mineral resource depletion) and economic preference (advantage give to the criteria related to energy use and cost).

Under all three criteria, the concrete RAC50 was either the sole optimal alternative or the optimal alternative together with RAC100 or NAC (in the environmental and economic preference scenarios, respectively). This result was also attributable to the very low cost of NAC and highlighted the need for economic measures to make RAC more attractive from a market perspective. In order to overcome this challenge, the following economic measures were identified as potentially leading to greater use of recycled aggregate and RAC:

- Increase of the tax on river aggregate extraction,
- Increase of the tax on landfilling construction and demolition waste, and
- Short-term subsidies for the recycling industry.

## 7. RECYCLED AGGREGATE CONCRETE IN THE NEW EUROCODE 2

The European Committee for Standardization (CEN) is currently finalizing development of a new Eurocode 2 for the design of concrete structures (prEN1992-1-1 [60]) which is currently under CEN Enquiry. The new design code will incorporate an informative annex for structural RAC. It is hoped that such an innovation will enable designers to safely and reliably design and construct RAC structures.

The provisions for RAC in prEN1992-1-1 are given in Annex N to which significant contributions were made through research carried out at the University of Belgrade's Faculty of Civil Engineering. An extensive background to Annex N can be found in the study by Tošić et al. [61] and an analysis of the RAC provision implications in Tošić et al. [62]. The work done in preparing the Annex N was based in large part on the previous experience of the research group of Prof. Snežana Marinković [33–35,25,26,47,63]. Herein, only a brief overview of Annex N is given.

Based on the recycled aggregate classification of EN 12620 [64] and EN 206 [65] (into Type A and Type B RA), a basic variable for RAC was defined as $\alpha_{RA}$, defined as the "quantity of fine and coarse recycled aggregate/total quantity of aggregate" (i.e. varying from 0 to 1). This way, the incorporation of fine RA (particle size ≤ 4 mm) with future revisions of EN 206 and EN 12620 is also facilitated.

For lower RA substitution ratios ($\alpha_{RA} \le 0.2$ for reinforced concrete, RC) it is assumed that there are no changes to RAC properties. For higher RA substitution ratios ($0.2 < \alpha_{RA} \le 0.4$ for RC, $\alpha_{RA} \le 0.2$ for prestressed concrete, PC), special provisions given in Table 8 may be applied. For even higher substitution ratios ($\alpha_{RA} > 0.4$ for RC and $\alpha_{RA} > 0.2$ for PC) properties of RAC should be measured. All of the above stated is valid for Type A RA (according to EN 206 [65]), whereas for Type B, the limiting substitution ratios should be decreased by 50%.

*Table 8 – Proposed provisions for RAC in Annex N of prEN1992-1-1*

| **RAC property** | **Correction for RAC** |
|---|---|
| Density | $\rho_{\mathrm{RAC}} = 2.50 - 0.22 \cdot \alpha_{\mathrm{RA}}$ |
| Modulus of elasticity | $E_{\mathrm{cm}} = k_{\mathrm{E}}.(1 - 0.25 \cdot \alpha_{\mathrm{RA}}) \cdot f_{\mathrm{cm}}^{1/3}$ |
| Shrinkage strain | $\varepsilon_{\mathrm{cs,RAC}} = (1 + 0.8 \cdot \alpha_{\mathrm{RA}}) \cdot \varepsilon_{\mathrm{cs}}$ |
| Creep coefficient | $\varphi_{\mathrm{RAC}} = (1 + 0.6 \cdot \alpha_{\mathrm{RA}}) \cdot \varphi$ |
| Peak strain | $\varepsilon_{\mathrm{c1}} = (1 + 0.33 \cdot \alpha_{\mathrm{RA}}) \cdot 0.7 \cdot f_{\mathrm{cm}}^{1/3} \leq 2.8‰$ |
| Ultimate strain | $\varepsilon_{\mathrm{cu1}} = (1 + 0.33 \cdot \alpha_{\mathrm{RA}}) \cdot [2.8 + 14 \cdot (1 - f_{\mathrm{cm}}/108)^4] \leq 3.5‰$ |
| Shear strength | $\tau_{\mathrm{Rd,c}} = (1 - 0.2 \cdot \alpha_{\mathrm{RA}}) \cdot \frac{0.66}{\gamma_{\mathrm{V}}} \cdot \left(100 \cdot \rho_{\mathrm{l}} \cdot f_{\mathrm{ck}} \cdot \frac{d_{\mathrm{dg}}}{d_{\mathrm{v}}}\right)^{1/3}$<br>$\tau_{\mathrm{Rdc,min}} = (1 - 0.2 \cdot \alpha_{\mathrm{RA}}) \cdot \frac{11}{\gamma_{\mathrm{V}}} \cdot \sqrt{\frac{f_{\mathrm{ck}}}{f_{\mathrm{yd}}} \frac{d_{\mathrm{dg}}}{d_{\mathrm{v}}}}$<br>The parameter $d_{\mathrm{dg}}$ taking account of concrete type and its aggregate properties shall be assumed as $d_{\mathrm{dg}}$ = 16 mm. |
| Deflection control | $\zeta = 1 - \beta_{\mathrm{tRA}} \cdot \left(\frac{\sigma_{\mathrm{sr}}}{\sigma_{\mathrm{s}}}\right)^2$<br>where<br>$\beta_{\mathrm{tRA}} = 1.0$ for single, short-term loading<br>$\beta_{\mathrm{tRA}} = 0.25$ for sustained or repeated loading |
| Concrete cover for durability | Determine exposure resistance by testing if relevant. For concrete including recycled aggregate, the same minimum cover depth for durability $c_{\mathrm{min,dur}}$ applies provided the material pertains the same exposure resistance class as concrete including natural aggregate only.<br>If exposure resistance is not determined, for reinforced concrete and for prestressed concrete when $\alpha_{\mathrm{RA}} > 0$, the values of $c_{\mathrm{min,dur}}$ should be increased by 5 mm for exposure to carbonation and 10 mm for exposure to chloride ingress |

$\rho_{\mathrm{RAC}}$ – density of RAC; $E_{\mathrm{cm}}$ – modulus of elasticity; $k_{\mathrm{E}}$ – factor dependent on the type of NA (can be taken as 9500);

$f_{\mathrm{cm}}$ – mean compressive strength of concrete; $\varepsilon_{\mathrm{cs,RAC}}$ – shrinkage strain of RAC; $\varepsilon_{\mathrm{cs}}$ – shrinkage strain of NAC;

$\varphi_{\mathrm{RAC}}$ – creep coefficient of RAC; $\varphi$ – creep coefficient of NAC; $\tau_{\mathrm{Rd,c}}$ – shear stress resistance of members without shear reinforcement;

$\gamma_{\mathrm{V}}$ –partial factor for shear resistance; $\rho_{\mathrm{l}}$ –longitudinal reinforcement ratio; $f_{\mathrm{ck}}$ – characteristic compressive strength of concrete;

$d_{\mathrm{dg}}$ – size parameter describing shear failure zone roughness; $d_{\mathrm{v}}$ – shear-resisting effective depth;

$\tau_{\mathrm{Rdc,min}}$ – minimum shear stress resistance; $\zeta$ – tension stiffening distribution coefficient; $\sigma_{\mathrm{sr}}$ – stress in tension reinforcement calculated on the basis of a cracked section under the loading conditions causing first cracking; $\sigma_{\mathrm{s}}$ – stress in tension reinforcement;

$c_{\mathrm{min,dur}}$ – minimum concrete cover due to durability requirements

As can be seen from the table, the largest impact of RA incorporation is on the RAC modulus of elasticity, shrinkage strain and creep coefficient. On the structural level, beside an effect on the reduction of the roughness zone in shear cracks, there is a reduction of tension stiffening that impacts deflection control. Finally, for durability, the new EC2 allows either the use of current environmental exposure class-based concrete covers or the use of a new performance-based classification based on “exposure resistance classes” (ERC). The use of ERCs means that concrete cover is directly determined based on the concrete resistance class. In that case, no changes in cover are necessary

for RAC if it belongs to the same ERC as NAC. Nonetheless, since countries will be able to opt out of the use of ERCs, provisions for increasing the minimum concrete cover due to durability are provided for exposures to carbonation and chloride ingress.

## 8. CONCLUSION

An extensive experimental and analytical research on several sustainable structural concrete solutions was performed by Concrete Structures Research Group at the Faculty of Civil Engineering in Belgrade. In particular, recycled aggregate concrete, high-volume fly ash concrete, alkali activated fly ash concrete as well as their combinations were investigated. Tests on material properties and structural behaviour under short and long-term loading on full-scale reinforced concrete beams were carried out, as well as sustainability assessments of the structural use of such concretes.

Generally, it can be concluded that it is possible to produce above mentioned green concretes with similar mix design and comparable mechanical properties to those of conventional concrete (made with only natural aggregates and cement binder). What however cannot be avoided is higher shrinkage and creep of RAC, and lower carbonation resistance of both RAC and HVFAC. Nevertheless, taking all this into account, sustainability assessments showed that investigated green concretes had better environmental performance, i.e. lower environmental impacts compared with conventional concrete. This is especially valid for combination of recycled aggregate and fly ash concrete which proved to be the best environmental option in performed assessments.

Based on databases compiled of own and other researchers' experimental results, and their analytical assessment, recommendations for the design of structural members including strength, serviceability and durability were proposed. However, since investigated green concretes include recycled and waste materials, there is a larger uncertainty regarding their properties and consequently the properties of concrete. This fact should be kept in mind when codifying design expressions which were developed on the basis of experimental and numerical research.

The new Eurocode 2 for the design of concrete structures (prEN1992-1-1), which is currently under CEN Enquiry, will incorporate an informative annex for structural RAC. The provisions for RAC are given in Annex N to which significant contributions were made through research carried out at the University of Belgrade's Faculty of Civil Engineering. It is hoped that such an innovation will enable designers to safely and reliably design and construct RAC structures.

Concrete gained a lot of negative connotation recently because of its impact on the environment and men's health. Large environmental impact of concrete comes from its large global production; in fact, the specific amount of harmful impacts embodied in concrete unit is, in comparison with other building materials, relatively small. It is true that many things on which men's future health and prosperity depend are today in jeopardy: climate stability, the resilience and productivity of natural systems, biodiversity. Urban growth certainly accelerates and enlarges the spread of negative impacts on the environment. Half of the world's population already lives in cities, with a strong growth rate. According to UN Population Division forecast more than six billion people will live in cities by 2050. There is no doubt that the demand for concrete will significantly increase in future, due to the rise of population and housing and infrastructure development needs, especially in Asia. On the other hand, no alternative for concrete as a major global construction material currently exists that can be applied at sufficient scale. That is why we need to raise trust in the use of green concrete solutions: on technology level through developing more efficient and cheaper production technologies; on economy level through implementing measures to stimulate the use; and on the social level, through transferring knowledge from science to industry and constant education about the benefits.

**REFERENCES**

[1] IPCC, 2014. AR5 Climate Change 2014: Impacts, Adaptation, and Vulnerability.

[2] 1IPCC, 2018. Global Warming of 1.5 ºC.

[3] United Nations, 2015. Paris Agreement: United nations framework convention on climate change. Paris, France.

[4] European Commission, 2016. The European construction sector: A global partner.

[5] N.D. Oikonomou, 2005. Recycled concrete aggregates. Cem. Concr. Compos. 27, 315–318.

[6] Eurostat, 2017. Generation of waste by waste category, hazardousness and NACE Rev. 2 activity. Luxembourg.

[7] European Parliament, 2018. Amending Energy Performance of Buildings Directive (2018/844/EU).

[8] WBCSD, 2009. The Cement Sustainability Initiative. World Bus. Counc. Sustain. Dev.

[9] Scrivener, K.L., et al., 2016. Eco-efficient cements: Potential, economically viable solutions for a low-CO2, cement based materials industry. Paris.

[10] I. Ignjatović, Ultimate strength of reinforced recycled aggregate concrete beams. University of Belgrade, 2013.

[11] S. Marinković, V. Radonjanin. M. Malešev, I. Ignjatović (2009): Reciklirani agregat u konstrukcijskim betonima - tehnologija, svojstva, primena, Savremeno graditeljstvo, Br. 02, s. 58-72, Banja Luka.

[12] I. Ignjatović, Aleksandar Savić, S. Marinković (2011): Eksperimentalno ispitivanje betona od recikliranog agregata, Građevinski kalendar 2011, Vol.43, s. 103-145.

[13] I. Ignjatović, A. Savić, S. Marinković: Analysis of modulus of elasticity determination in recycled aggregate concrete, Proceedings of the XXV Congress and International Symposium, DIMK Srbije, pp. 461-470, Tara, October 19-21, 2011.

[14] I. Ignjatović, S. Marinković: Creep and shrinkage of recycled aggregate concrete, Proceedings of the 13th International Symposium of MASE, Ohrid, Macedonia, pp. 201-206, September 14-17, 2009.

[15] N. Tošić, I. Ignjatović, D. Jevtić, J. Dragaš (2013): Shrinkage of Recycled Aggregate Concrete, Tehnika – Naše građevinarstvo, 67(5).

[16] S. Marinković, V. Radonjanin, M. Malešev, I. Ignjatović: Properties and environmental impact of recycled aggregate concrete for structural use, Proceedings of Seminar of COST action C25: Sustainability of Constructions-Integrated Approach to Life-time Structural Engineering, pp. 225-236, Timisoara, Romania, October 23-24, 2009.

[17] S. Marinković, V. Radonjanin, M. Malešev, I. Ignjatović: Sustainable concrete construction: recycled aggregate concrete for structural use, Summary Report of the Cooperative Activities of the COST Action C25: Volume 1 Sustainability of Constructions - Integrated Approach towards Sustainable Constructions, pp. 189-204, Innsbruck, Austria, February 3-5, 2011.

[18] S. Marinković, V. Radonjanin, M. Malešev, I. Ignjatović: Data sheet for recycled aggregate concrete, Summary Report of the Cooperative Activities of the COST Action C25: Volume 1 Sustainability of Constructions - Integrated Approach Towards Sustainable Constructions, pp. 497-501, Innsbruck, Austria, February 3-5, 2011.

[19] Ignjatović I., Tošić N., Marinković S., Dragaš J. Tehnološki i ekonomski aspekt proizvodnje agregata od recikliranog betona u Srbiji. In: Građevinski materijali u savremenom graditeljstvu. DIMK. Beograd, 2015

[20] S. Marinković, I. Ignjatović, A. Terzić, Lj. Pavlović (2009): Mikrostruktura i trajnost betona sa

recikliranim agregatom, Izgradnja 63, Br.11-12, s. 523-533.

[21] I. Ignjatović, S. Marinković, A. Savić: Projektovanje sastava betona sa agregatom od recikliranog betona, IV Internacionalni naučno-stručni skup Građevinarstvo – nauka i praksa, Gradjevinski fakultet u Podgorici, pp. 1055-1062, februar 20-24, 2012.

[22] I. Ignjatović, S. Marinković: Ponašanje pri savijanju greda od betona na bazi recikliranog agregata, Zbornik radova Simpozijuma DGKS, s. 465-471, Zlatibor, 24-26. septembar, 2008.

[23] S. Marinković, I. Ignjatović: Ponašanje pri smicanju greda od betona na bazi recikliranog agregata, Zbornik radova Simpozijuma o istraživanjima i primeni savremenih dostignuća u našem građevinarstvu u oblasti materijala i konstrukcija DIMK Srbije, s. 225-234, Divčibare, 15-17. oktobar, 2008.

[24] I. Ignjatović, S. Marinković, N. Tošić (2015) Flexural performance of reinforced recycled aggregate and natural aggregate beams - experimental, analytical and numerical comparison. In: International Conference on Sustainable Structural Concrete. La Plata, Argentina, 2015

[25] I. Ignjatović, S. Marinković, Z. Mišković, A. Savić, Flexural behavior of reinforced recycled aggregate concrete beams under short-term loading, Materials and Structures. 2013; 46(6), 1045-1059. https://doi.org/10.1617/s11527-012-9952-9

[26] I. Ignjatović, S. Marinković, N. Tošić, Shear behaviour of recycled aggregate concrete beams with and without shear reinforcement. Engineering Structures. 2017; 141, 386-401. http://dx.doi.org/10.1016/j.engstruct.2017.03.026

[27] CEN, EN 1992-1-1, in: CEN (Ed.), 1st ed., ISS, Belgrade, 2015.

[28] ACI Committee 318. Building Code Requirements for Structural Concrete (ACI 318-11) and Commentary. Farmington Hills, MI: American Concrete Institute; 2011.

[29] N. Tošić, Behaviour of reinforced concrete beams made with recycled and waste materials under long-term loading, University of Belgrade, 2018.

[30] N. Tošić, S. Marinković, N. Pecić, I. Ignjatović, J. Dragaš, Long-term behaviour of reinforced beams made with natural or recycled aggregate concrete and high-volume fly ash concrete, Constr. Build. Mater. 176 (2018) 344–358. https://doi.org/10.1016/j.conbuildmat.2018.05.002.

[31] C.Q.C.-Q. Lye, R.K.R.K. Dhir, G.S.G.S. Ghataora, R.K.R.K. Dhir, Shrinkage of recycled aggregate concrete, in: Struct. Build. Proc. Inst. Civ. Eng., ICE, 2016: pp. 1–25. https://doi.org/10.1680/jstbu.15.00138.

[32] R.V. V. Silva, J. De Brito, R.K.K. Dhir, Prediction of the shrinkage behavior of recycled aggregate concrete: A review, Constr. Build. Mater. 77 (2015) 327–339. https://doi.org/10.1016/j.conbuildmat.2014.12.102.

[33] N. Tošić, A. de la Fuente, S. Marinković, Shrinkage of recycled aggregate concrete: experimental database and application of fib Model Code 2010, Mater. Struct. Constr. 51 (2018) 126. https://doi.org/10.1617/s11527-018-1258-0.

[34] N. Tošić, A. de la Fuente, S. Marinković, Creep of recycled aggregate concrete: Experimental database and creep prediction model according to the fib Model Code 2010, Constr. Build. Mater. 195 (2019) 590–599. https://doi.org/10.1016/j.conbuildmat.2018.11.048.

[35] N. Tošić, S. Marinković, J. de Brito, Deflection control for reinforced recycled aggregate concrete beams: Experimental database and extension of the fib Model Code 2010 model, Struct. Concr. 20 (2019) 2015–2029. https://doi.org/10.1002/suco.201900035.

[36] FIB, fib Model Code for Concrete Structures 2010, International Federation for Structural Concrete (fib), Lausanne, 2013. https://doi.org/10.1002/9783433604090.

[37] A.M. Knaack, Y.C. Kurama, Sustained Service Load Behavior of Concrete Beams with Recycled Concrete Aggregates, ACI Struct. J. 112 (2015) 565–578. https://doi.org/10.14359/51687799.

[38] S. Seara-Paz, B. González-Fonteboa, F. Martínez-Abella, I. González-Taboada, Time-dependent behaviour of structural concrete made with recycled coarse aggregates. Creep and shrinkage, Constr. Build. Mater. 122 (2016) 95–109. https://doi.org/10.1016/j.conbuildmat.2016.06.050.

[39] ASTM C618-12a, 'Standard Specification for Coal Fly Ash and Raw or Calcined Natural Pozzolan for Use in Concrete', ASTM International, West Conshohocken, 2012.

[40] EN 450-1:2010, Fly ash for concrete – Part 1: Definition, specifications and conformity criteria, CEN, Brussels, 2010.

[41] J. Dragaš, N. Tošić, I. Ignjatović, S. Marinković, Mechanical and timedependent properties of high-volume fly ash concrete for structural use, Mag. Concr. Res. 68 (2016), 632–645.

[42] I. Ignjatović, Z. Sas, J. Dragaš, J. Somlai, T. Kovacs, Radiological and material characterization of high volume fly ash concrete, J. Environ. Radioact. 168 (2017), 38-45.

[43] J. Dragaš, S. Marinković, V. Radonjanin, Prediction models for high-volume fly ash concrete practical application: mechanical properties and experimental database, Building Materials and Structures 64 (2021) 19-43.

[44] J. Dragaš, Ultimate capacity of high volume fly ash reinforced concrete beams, University of Belgrade, 2018.

[45] C. Nuccetelli, R. Trevisi, I. Ignjatović, J. Dragaš, Alkali-activated concrete with Serbian fly ash and its radiological impact, J. Environ. Radioact. 168 (2017), 168, 30-37.

[46] B. Pailes, Effect of Cracking on Reinforced Concrete Corrosion, ACI Spring 2018 Conv. (2018). https://www.concrete.org/education/freewebsessions/completelisting/coursepreviews.aspx?ID=51713407 (accessed March 10, 2019).

[47] V. Carević, I. Ignjatović, Evaluation of concrete cover depth for green concretes exposed to carbonation, Struct. Concr. (2020). doi:10.1002/suco.202000086.

[48] V. Carević, Uticaj Prslina na Mehanizme Deterioracije i Trajnost Armiranobetonskih Konstrukcija, PhD Thesis, University of Belgrade, Faculty of Civil Engineering, 2020.

[49] V. Carević, I. Ignjatović, J. Dragaš, Model for practical carbonation depth prediction for high volume fly ash concrete and recycled aggregate concrete, Constr. Build. Mater. 213 (2019) 194–208. doi:10.1016/j.conbuildmat.2019.03.267.

[50] fib-Bulletin 34, Model Code for Service Life Design, 1st ed., International Federation for Structural Concrete (fib), Lausanne, Switzerland, 2006.

[51] S. Marinković, V. Carević, J. Dragaš, The role of service life in Life Cycle Assessment of concrete structures, J. Clean. Prod. 290 (2021) 125610. doi:10.1016/j.jclepro.2020.125610.

[52] V. Carević, I. Ignjatović, Influence of loading cracks on the carbonation resistance of RC elements, Constr. Build. Mater. 227 (2019) 116583. doi:10.1016/j.conbuildmat.2019.07.309.

[53] V. Carević, Ignjatović Ivan, Influence of cracks on the carbonation resistance of concrete structures, in: E. Júlio, J. Valença, A.S. Louro (Eds.), Proc. Fib Symp. Concr. Struct. New Trends Eco-Efficiency Perform., International Federation for Structural Concrete (fib), Lisbon, Portugal, 2021: pp. 422–431.

[54] S. Marinković, V. Radonjanin, M. Malešev, I. Ignjatović, Comparative environmental assessment of natural and recycled aggregate concrete, Waste Management 30 (2010) 2255-2264.

[55] S. Marinković, J. Dragaš, I. Ignjatović, N. Tošić, Environmental assessment of green concretes for structural use, J. Clean. Prod. 154 (2017) 633-649.

[56] S. Marinković, V. Radonjanin, M. Malešev, I. Lukić, Life Cycle Environmental Impact Assessment of Concrete, in L. Braganca et al (eds):. Sustainability of Constructions -

Integrated Approach to Life-time Structural Engineering, Proc. Cost C25, 2008: pp. 3.5-3.16.

[57] J.B Guinée, M Gorrée, R. Heijungs, G. Huppes, R. Kleijn, A. de Koning, L. van Oers, A. Wegener Sleeswijk, S. Suh, H.A. Udo de Haes, et al. Handbook on Life Cycle Assessment. Operational Guide to the ISO Standards. I: LCA in Perspective. IIa: Guide. IIb: Operational Annex. III: Scientific Background; Kluwer Academic Publishers: Dordrecht, The Netherlands, 2002; ISBN 1-4020-0228-9.

[58] L. Diaz-Balterio, C. Romero, In a search of a natural systems systainabilitz index, Ecol. Econ. 49 (2004) 401–405.

[59] Tošić, Nikola, Snežana Marinković, Tina Dašić, and Miloš Stanić. "Multicriteria optimization of natural and recycled aggregate concrete for structural use." Journal of Cleaner Production 87 (2015): 766-776.

[60] prEN1992-1-1, Eurocode 2: Design of concrete structures – Part 1-1: General rules, rules for buildings, bridges and civil engineering structures, CEN, Brussels, 2021.

[61] N. Tošić, J.M.J.M. Torrenti, T. Sedran, I. Ignjatović, Toward a codified design of recycled aggregate concrete structures: Background for the new fib Model Code 2020 and Eurocode 2, Struct. Concr. (2020) 1–23. https://doi.org/10.1002/suco.202000512.

[62] N. Tošić, J.M. Torrenti, New Eurocode 2 provisions for recycled aggregate concrete and their implications for the design of one-way slabs, Build. Mater. Struct. 64 (2021) 119–125. https://doi.org/10.5937/GRMK2102119T.

[63] N. Tošić, S. Marinković, I. Ignjatović, A database on flexural and shear strength of reinforced recycled aggregate concrete beams and comparison to Eurocode 2 predictions, Constr. Build. Mater. 127 (2016) 932–944. https://doi.org/10.1016/j.conbuildmat.2016.10.058.

[64] EN 12620, Aggregates for concrete, CEN, Brussels, 2013.

[65] EN 206, Concrete - Specification, performance, production and conformity, CEN, Brussels, 2013.